February 2017

FINAL REPORT

Preliminary Feasibility Study for South San Francisco Bay Shoreline Economic Impact Areas 1–10
Appendix I: Long Wave Modeling Report

Prepared for
Santa Clara Valley Water District
5750 Almaden Expressway
San Jose, California 95118-3686

Prepared by
Anchor QEA, LLC
130 Battery Street, Suite 400
San Francisco, California 94111

Santa Clara Valley Water District

ANCHOR QEA

PRELIMINARY FEASIBILITY STUDY FOR SOUTH SAN FRANCISCO BAY SHORELINE ECONOMIC IMPACT AREAS 1-10 LONG WAVE MODELING REPORT

FINAL REPORT

Prepared for

Santa Clara Valley Water District
5750 Almaden Expressway
San Jose, California 95118-3686

Prepared by

Anchor QEA, LLC
130 Battery Street, Suite 400
San Francisco, California 94111

February 2017

TABLE OF CONTENTS

LIST OF ACRONYMS AND ABBREVIATIONS

1-D	one-dimensional
2-D	two-dimensional
3-D	three-dimensional
BAAQMD	Bay Area Air Quality Management District
cfs	cubic feet per second
CCWD	Contra Costa Water District
CIMIS	California Irrigation Management Information System
DEM	Digital Elevation Model
DICU	Delta Island Consumptive Use
DWR	Department of Water Resources
EIA	Economic Impact Area
ft	foot
ICS	Inner Charleston Slough
IPCC	Intergovernmental Panel on Climate Change
m	meter
MAT	maximum annual tide
MLLW	mean lower low water
mph	miles per hour
MSL	mean sea level
NAVD88	North American Vertical Datum of 1988
NOAA	National Oceanic and Atmospheric Administration
NRC	National Research Council
NTDE	National Tidal Datum Epoch
PAFB	Palo Alto Flood Basin
s	second
SCVWD	Santa Clara Valley Water District
SFPORTS	San Francisco Physical Oceanographic Real-Time System

SLR	sea level rise
SSC	suspended solids concentration
SSFBSS	South San Francisco Bay Shoreline Study
TRIM	Tidal, Residual, Intertidal & Mudflat Model
UnTRIM	Unstructured Tidal, Residual, Intertidal & Mudflat Model
USACE	U.S. Army Corps of Engineers
USGS	United States Geological Survey
WARMER	Wetland Accretion Rate Model for Ecosystem Resilience
yr	year

1 INTRODUCTION

This report documents the three-dimensional (3-D) hydrodynamic modeling conducted for the preliminary feasibility study for South San Francisco Bay Shoreline Economic Impact Areas (EIAs) 1-10. This report is divided into the following seven major sections:

- **Section 1. Introduction.** This section provides a summary of the scope and organization of the report.
- **Section 2. Long Wave Modeling Overview.** This section provides a brief overview of the project study area, project approach, and project objectives.
- **Section 3. UnTRIM Bay-Delta Model Description**. This section provides a brief description of the Unstructured Tidal, Residual, Intertidal & Mudflat (UnTRIM) hydrodynamic model and the UnTRIM Bay-Delta model, as well as a description of the data sources used to develop the model bathymetry for this study.
- **Section 4. Model Boundary Conditions for Scenario Simulations.** This section describes the assumptions and model boundary conditions used to develop the matrix of wind, flow, and tide forcing parameters used in the scenario simulations.
- **Section 5. Simulation of Existing Conditions for Year 0 and Year 50.** This section describes the scenario assumptions and results of the model scenario simulations under existing conditions for both Year 0 and Year 50.
- **Section 6. Simulation of With-Project Conditions for Year 0 and Year 50.** This section describes the scenario assumptions and results of the model scenario simulations under with-project conditions for both Year 0 and Year 50.
- **Section 7. Summary and Conclusions.** This section presents a summary of the modeling conducted in this study and the conclusions drawn from this work.

2 LONG WAVE MODELING OVERVIEW

The preliminary feasibility study for South San Francisco Bay Shoreline EIAs 1-10 is being conducted for the Santa Clara Valley Water District (SCVWD) in collaboration with Noble Consultants. The primary purpose of the preliminary feasibility study is to determine the necessary levee heights to protect infrastructure in the Far South San Francisco Bay. The purpose of the long wave modeling component of the study is to provide predictions of maximum water surface elevations and wind setup for a suite of synthesized events spanning a wide range of hydrodynamic conditions which can be used in Monte Carlo simulations to develop flood risk frequency curves along the project levee under both existing and with-project conditions.

2.1 Study Area

The study area is located south of Dumbarton Bridge at the far southern end of San Francisco Bay, from San Francisquito Creek to Guadalupe River (Figure 2-1). The study area includes South Bay Salt Ponds A1 through A8, which were previously used for salt production by Cargill, Inc, and which are currently undergoing restoration as part of the South Bay Salt Pond Restoration Project.

Figure 2-1
South San Francisco Shoreline Study project area for EIAs 1-10

2.2 Project Objectives

The primary objective of the long wave modeling component of the project is to provide predictions of water levels for a set of synthesized events that cover the ranges of all the controlling parameters, such as tide, residual, wind speed, and wind direction under existing conditions and with-project conditions for both Year 0 and Year 50. The predicted maximum water surface elevations spanning the range of conditions evaluated for this project were provided in lookup tables suitable for use in Monte Carlo simulations conducted by Noble Consultants. The results of the Monte Carlo simulations were used to establish flood stage frequency curves for each set of conditions evaluated. The results of the Monte Carlo analysis are documented in a separate report prepared by Noble Consultants.

2.3 Modeling Approach

The UnTRIM Bay-Delta model is a 3-D hydrodynamic model of San Francisco Bay and the Sacramento-San Joaquin Delta, developed using the UnTRIM hydrodynamic model (MacWilliams et al. 2007, 2008, 2009, 2015). The UnTRIM Bay-Delta model extends from the Pacific Ocean through the entire Sacramento-San Joaquin Delta. As part of the South San

Francisco Bay Shoreline Study (SSFBSS), a high-resolution model grid of the project site was developed using a high resolution Digital Elevation Model (DEM) of the project area developed by the U.S. Army Corps of Engineers (USACE), San Francisco District (MacWilliams et al. 2012). This high-resolution grid of the project area was merged into the existing model grid of the San Francisco Bay-Delta.

The model grid developed for the SSFBSS (MacWilliams et al. 2012) included a high-resolution grid for Far South San Francisco Bay and the South Bay Salt Ponds, but did not extend landward of the existing levees. As part of the current study for EIAs 1-10, the model grid was extended behind the project levees and further upstream along the Bay tributaries in EIAs 1-10 to allow for the evaluation of scenarios under which the existing levee failed or overtopped, and for the prediction of water levels behind the levees.

3 UNTRIM BAY-DELTA MODEL DESCRIPTION

The hydrodynamic model used in this technical study is the 3-D hydrodynamic model UnTRIM (Casulli and Zanolli 2002). A complete description of the governing equations, numerical discretization, and numerical properties of UnTRIM are described in Casulli and Zanolli (2002, 2005), Casulli (1999), and Casulli and Walters (2000).

The UnTRIM model solves the 3-D Navier-Stokes equations on an unstructured grid in the horizontal plane. The boundaries between vertical layers are at fixed elevations, and cell heights can be varied vertically to provide increased resolution near the surface or other vertical locations. Volume conservation is satisfied by a volume integration of the incompressible continuity equation, and the free surface is calculated by integrating the continuity equation over the depth, and using a kinematic condition at the free surface as described in Casulli (1990). The numerical method allows full wetting and drying of cells in the vertical and horizontal directions. The governing equations are discretized using a finite difference-finite volume algorithm. Discretization of the governing equations and model boundary conditions are presented in detail by Casulli and Zanolli (2002). All details and numerical properties of this state-of-the-art 3-D model are well-documented in the peer reviewed literature (Casulli and Zanolli 2002, 2005).

3.1 Turbulence Model

The turbulence closure model used in the present study is a two-equation model comprised of a turbulent kinetic energy equation and a generic length-scale equation. The parameters of the generic length-scale equation are chosen to yield the k-ε closure (Umlauf and Burchard 2003). The Kantha and Clayson (1994) quasi-equilibrium stability functions are used. All parameter values used in the k-ε closure are identical to those used by Warner et al. (2005), including the minimum eddy diffusivity and eddy viscosity values, which were $5x10^{-6}$ m^2 s^{-1}. The numerical method used to solve the equations of the turbulence closure is a semi-implicit method that results in tridiagonal positive-definite matrices in the water column of each grid cell and ensures that the turbulent variables remain positive (Deleersnijder et al. 1997).

3.2 Previous Applications

The Tidal, Residual, Intertidal & Mudflat (TRIM) 3-D model (Casulli and Cheng 1992) and UnTRIM model have been applied previously to San Francisco Bay (Cheng and Casulli 2002; MacWilliams and Cheng 2007; MacWilliams and Gross 2007; MacWilliams et al. 2007, 2008, 2015). The TRIM3D model (Casulli and Cattani 1994), which follows a similar numerical approach on structured horizontal grids, has been widely applied in San Francisco Bay (e.g., Cheng et al. 1993; Cheng and Casulli 1996; Gross et al. 1999, 2006), and a two-dimensional (2-D) version, TRIM2D, was used in the San Francisco Bay Physical Oceanographic Real-Time System (Cheng and Smith 1998). Thus, the UnTRIM numerical approach has been well-tested in San Francisco Bay and is very well suited for the modeling conducted for this study.

3.3 UnTRIM Bay-Delta Model

The UnTRIM Bay-Delta model extends from the Pacific Ocean through the entire Sacramento-San Joaquin Delta (Figure 3.3-1). The UnTRIM Bay-Delta model takes advantage of the grid flexibility allowed in an unstructured mesh by gradually varying grid cell sizes, beginning with large grid cells in the Pacific Ocean and gradually transitioning to finer grid resolution in the smaller sloughs, tidal channels, and creeks in the project area. This approach offers significant advantages both in terms of numerical efficiency and accuracy, and allows for local grid refinement for detailed analysis of local hydrodynamics, while still incorporating the overall hydrodynamics of the larger estuary in a single model.

The UnTRIM Bay-Delta model has been calibrated using water level, flow, and salinity data collected in San Francisco Bay and the Sacramento-San Joaquin Delta (MacWilliams et al. 2008, 2009, 2015). Predicted water levels were compared to observed water levels at National Oceanic and Atmospheric Administration (NOAA) and Department of Water Resources (DWR) stations in San Francisco Bay, and DWR and United States Geological Survey (USGS) flow and stage monitoring stations in the Sacramento-San Joaquin Delta. Predicted water levels in South San Francisco Bay were extensively validated as part of the Long Wave Modeling for the SSFBSS (MacWilliams et al. 2012).

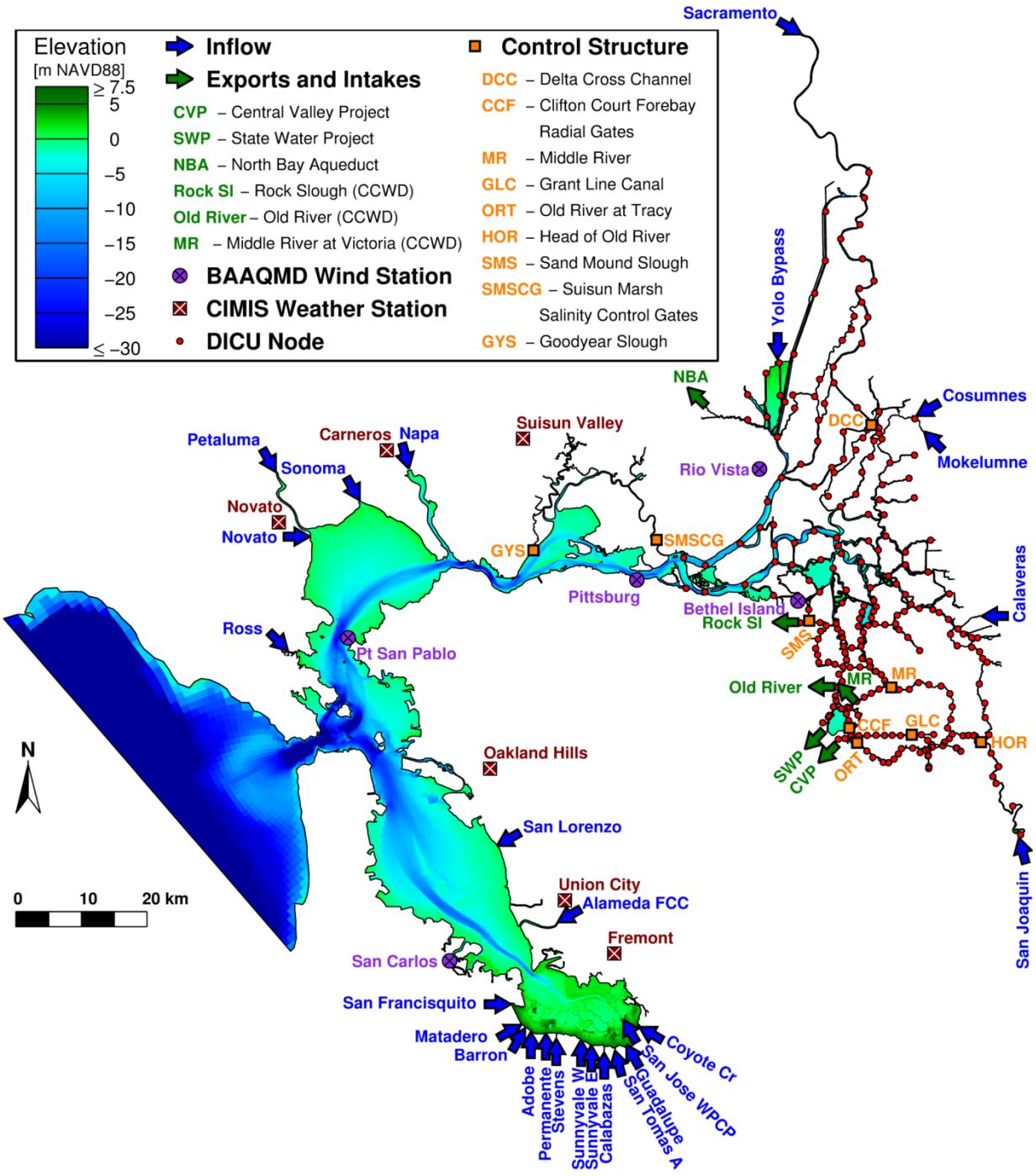

Figure 3.3-1

UnTRIM Bay-Delta model domain, bathymetry, and locations of model boundary conditions which include inflows, export facilities, intakes for the Contra Costa Water District (CCWD), wind stations from the Bay Area Air Quality Management District (BAAQMD), evaporation and precipitation from California Irrigation Management Information System (CIMIS) weather stations, Delta Island Consumptive Use (DICU), and flow control structures.

3.4 South San Francisco Bay Model Grid and Bathymetry Refinements

As part of the SSFBSS, the UnTRIM Bay-Delta model was refined to include a high-resolution model grid in the study area (MacWilliams et al. 2012). The model grid was developed using the grid generator JANET (Lippert and Sellerhoff 2007), and used quadrilateral cells aligned with the main channels in the project area. Pond and marsh areas were filled using triangular elements to allow for the grid to be exactly aligned to the levees surrounding each creek in the project area and the numerous salt ponds in the South Bay (Figure 3.4-1).

As part of the current study, the model grid was further expanded to include the areas landward of the levee in EIA 1 through EIA 10 that were potentially susceptible to flooding. The model grid was extended landward to an elevation of approximately 16 to 18 feet (ft) North American Vertical Datum of 1988 (NAVD88) (Figure 3.4-2). Following the approach used in the SSFBSS, quadrilateral cells aligned with the creeks and creek levees were used to extend the channels upstream, and urban area were filled using triangular elements.

The resulting model grid for the region south of Dumbarton Bridge (Figure 3.4-3) includes a total of 301,195 horizontal grid cells. There are more horizontal grid cells south of Dumbarton Bridge in this mesh than were used in the entire grid of the San Francisco Bay-Delta by MacWilliams et al. (2009; 2015). The combined mesh, which incorporates the high-resolution Far South Bay model into the high-resolution San Francisco Bay-Delta model, consists of 437,968 horizontal grid cells and 2.2 million 3-D cells. This extremely high-resolution mesh allows for resolution of detailed bathymetric features within the project area, including, for example, subtidal channels in the Alviso Island Ponds (Figure 3.4-4).

The UnTRIM Bay-Delta model was also refined to include the most recent available high-resolution bathymetric data in the project area. A high-resolution DEM of the project area was developed by the USACE, San Francisco District, using the data sources shown in Figure 3.4-5. This DEM was applied to the high-resolution mesh to provide the most accurate possible representation of the project area for this study. Levee crest elevations for the ten creeks in the study area were taken from HEC-RAS models of each creek provided by SCVWD (Noble Consultants 2009; 2015).

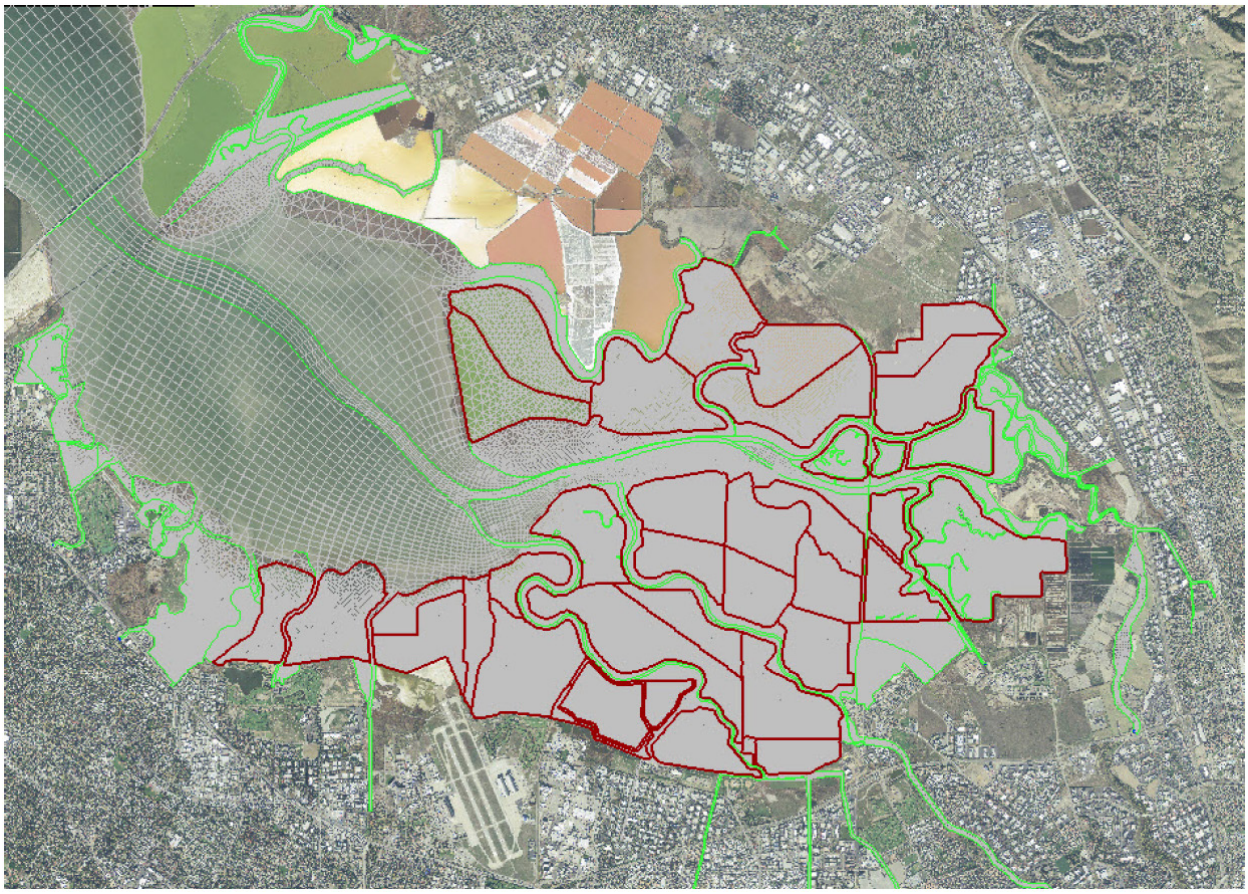

Figure 3.4-1

The UnTRIM model grid for the South San Francisco Bay Shoreline Study (MacWilliams et al. 2012) showing channel features (green) and levees (dark red) which are aligned with the model grid.

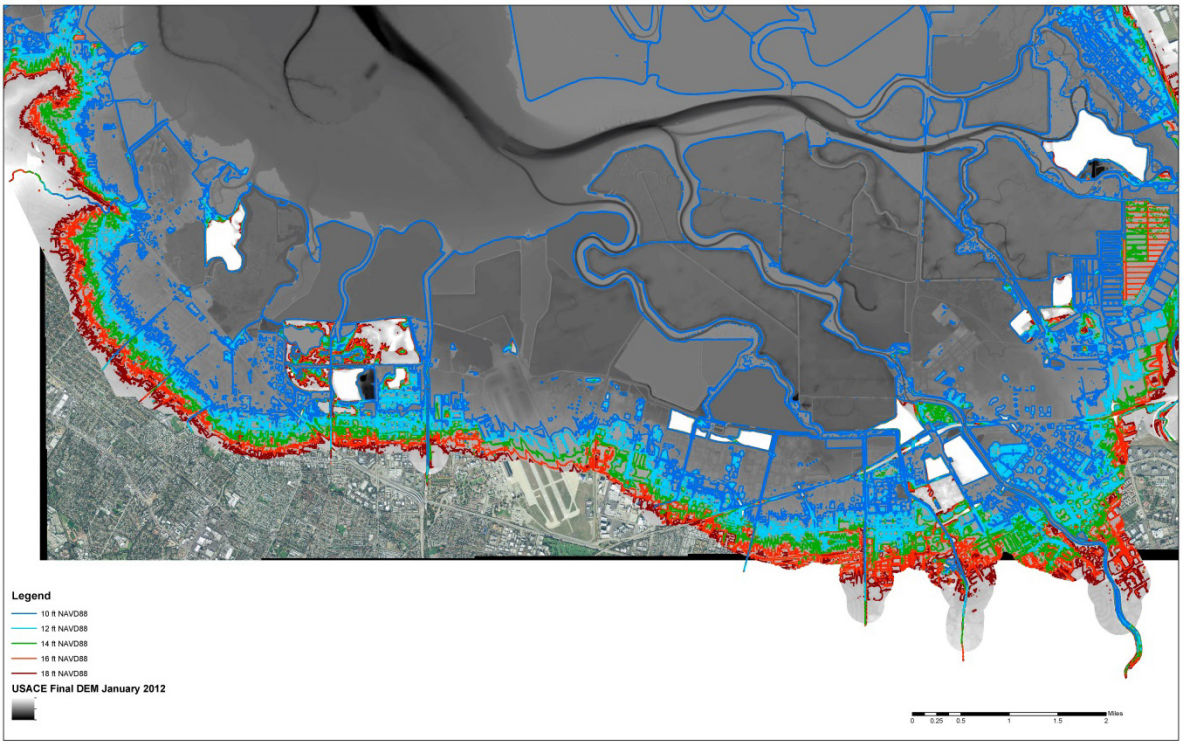

Figure 3.4-2

Far South Bay bathymetry showing contours at 2 ft intervals between 10 ft NAVD88 (blue) and 18 ft NAVD88 (dark red)

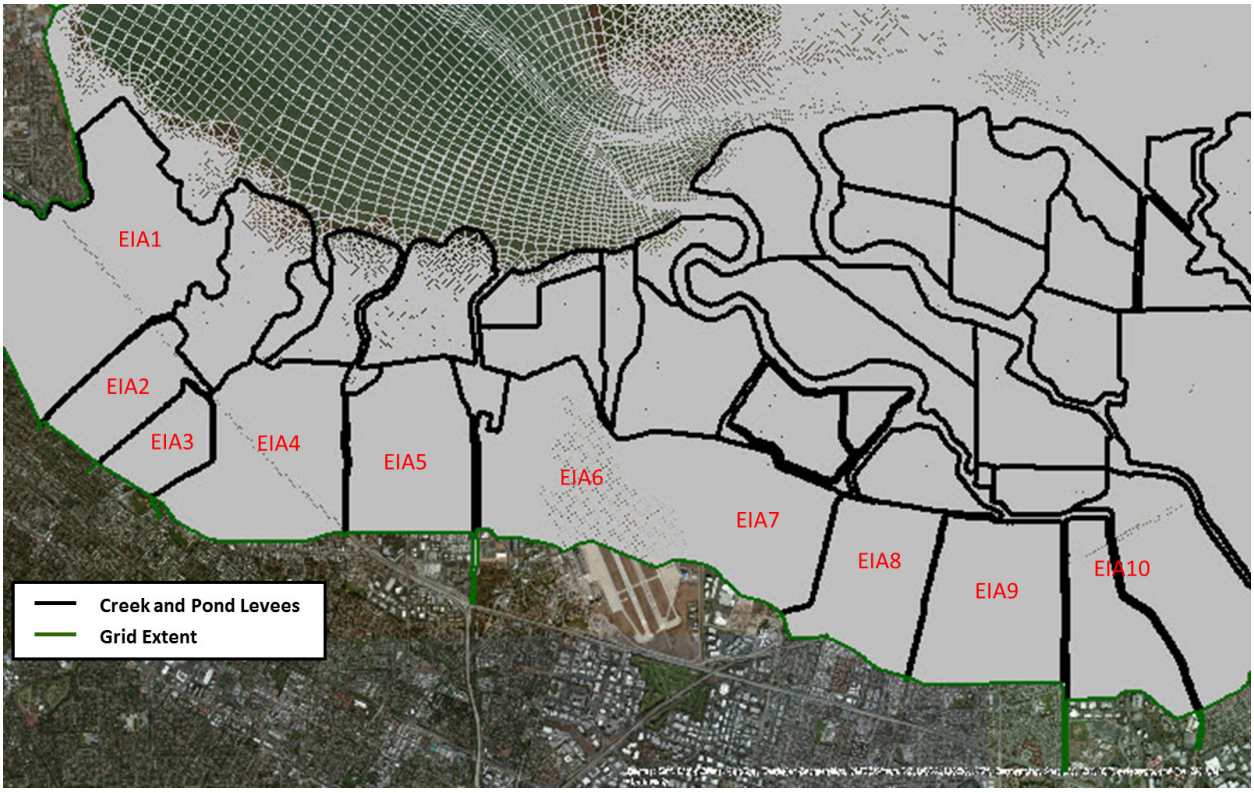

Figure 3.4-3

The UnTRIM model grid extent in EIA 1-10, which includes areas landward of the project levee

Figure 3.4-4
UnTRIM model grid in the vicinity of the Alviso Island ponds showing channel features (green) and levees (dark red) which are aligned with the model grid (from MacWilliams et al. 2012)

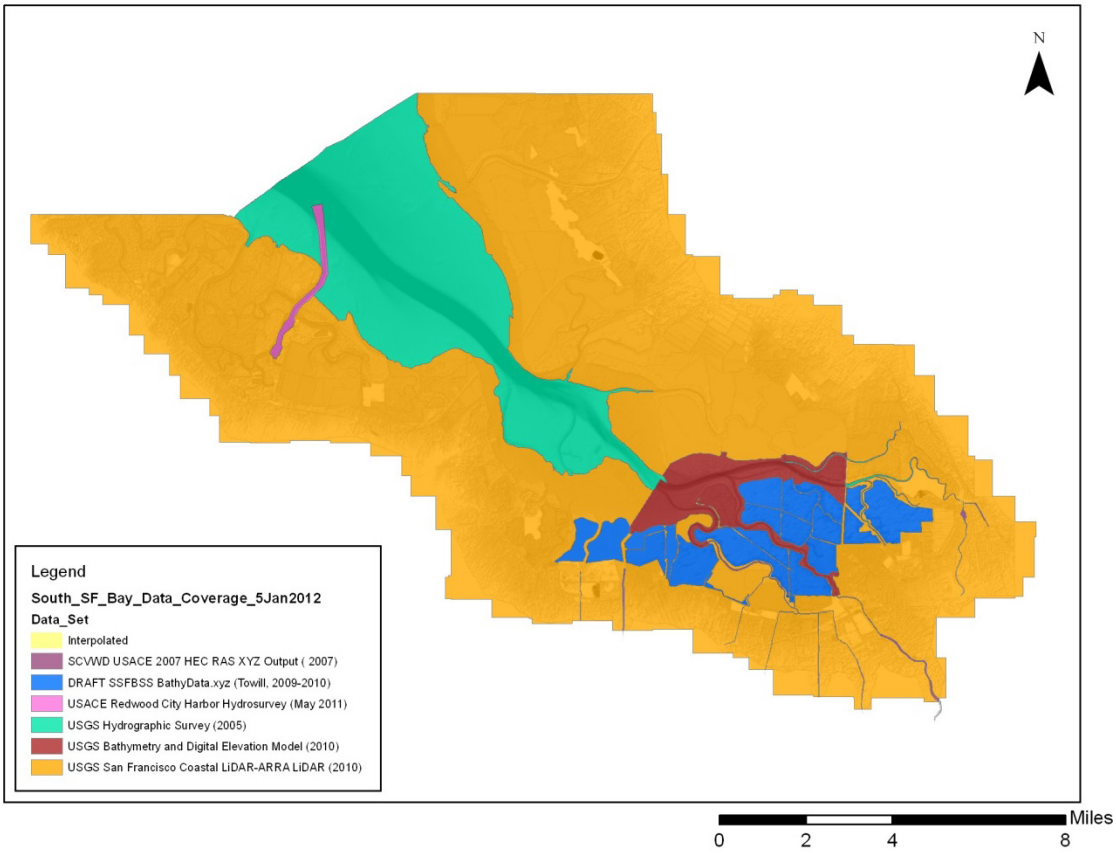

Figure 3.4-5
Data sets used in development of a high-resolution DEM of the Far South San Francisco Bay (Source: USACE)

3.5 South San Francisco Bay Model Calibration and Validation

As part of the SSFBSS (MacWilliams et al. 2012), extensive model calibration and validation was conducted within the study area. The model was calibrated using observed water level data during periods with the most extensive spatial availability of water level observations in the project area in 2005 and 2011. The model was validated using peak water level data from five separate storm periods between 1983 and 2006. These simulation periods include ten of the 47 highest observed water levels during storm events based on a ranking of the maximum verified tide data water level at the San Francisco NOAA tide station (9414290), including all of the top five ranked events. Because the only change to the model for this study was to extend the model grid to include the area behind the project levees and no changes were made to Bay or salt pond portions of the model domain, no further model validation was conducted as part of this study.

4 MODEL BOUNDARY CONDITIONS FOR SCENARIO SIMULATIONS

Model boundary conditions were developed for simulating both Year 0 and Year 50 conditions. For purposes of this study, 2017 is considered the base year (Year 0), and 2067 is used for Year 50 conditions. The same assumptions for Year 0 and Year 50 were made as part of the SSFBSS (MacWilliams et al. 2012). The model boundary conditions were developed to predict peak water levels for a set of synthesized events that cover the ranges of all the controlling parameters, such as tide, residual, wind speed, and wind direction in the project area. This section presents the model boundary conditions and assumptions used in the development of the long wave scenario simulations. These scenario simulations were used to develop lookup tables which provide the peak water level for each of the events at a set of evaluation locations in the project area. The same river and creek inflows and wind boundary conditions were used for Year 0 and Year 50. However, the tidal boundary conditions for Year 0 and Year 50 included different levels of SLR.

4.1 Tidal Boundary Conditions

A suite of tidal boundary conditions were developed to span the range of astronomical and residual tides observed at San Francisco (9414290). Based on an analysis of historical astronomic tides generated from tidal harmonic constituents and hourly water level observations at San Francisco (MacWilliams et al. 2012), the peak astronomic tides ranged from 5.15 to 7.25 feet mean lower low water (MLLW). The coincident residual associated with these peaks ranged from 0 to 2.4 feet. In order to provide a lookup table spanning the full range of possible conditions, four peak astronomic tides between 5.15 and 7.25 feet MLLW and three peak residual heights between 0.5 and 2.5 feet were selected (Table 4-1), resulting in a total of twelve event permutations with peak water levels at San Francisco (9414290).

For each astronomical tide peak, a historical event period was selected from the astronomical tides generated from tidal harmonic constituents at San Francisco (9414290) from the period between 1901 and 2005 such that the peak astronomical tide matched the target and the peak astronomical tide for the preceding three days did not exceed this peak water level. This ensured that a peak water level during the spin-up period prior to the event did not exceed

the event peak. These astronomical tides generated from tidal harmonic constituents were used to develop the synthetic events.

Each synthetic event spans a period of five days, from January 1, 2017 through January 5, 2017. For each event, the peak astronomical tide from the corresponding time series generated from the tidal harmonic constituents was shifted in time to occur at 12:00 on January 4, 2017. Each storm event spans a 48-hour period from January 3, 2017 at 12:00 to January 5, 2017 at 12:00, with the peak residual for each event occurring at 12:00 on January 4, 2017 which is coincident with the peak astronomical tide. The storm residual was represented by the first half cycle of a sine function with a period of 4 days and amplitude of between 0.5 and 2.5 feet. Figure 4.1-1 shows the resulting tides for events 1 through 3 (Table 4-1), developed using a peak astronomical tide of 5.15 feet. The resulting tides for events 4 through 6 (Table 4-1), developed using a peak astronomical tide of 5.85 feet, are shown on Figure 4.1-2. Figure 4.1-3 shows the resulting tides for events 7 through 9 (Table 4-1), developed using a peak astronomical tide of 6.55 feet. The resulting tides for events 10 through 12 (Table 4-1), developed using a peak astronomical tide of 7.25 feet, are shown on Figure 4.1-4. For the model ocean boundary, the synthetic tides developed at San Francisco (9414290) for each of the 12 events simulated were multiplied by an amplification factor to account for the difference in tidal range between observed San Francisco tides and tides along the model ocean boundary. A phase lead was also applied to account for the phase difference between the San Francisco tide station and the model boundary. These adjustments ensured that the resulting peak water surface elevation predicted at the NOAA San Francisco station for each of the simulations was within 0.018 feet of the peak values shown in Table 4-1.

Table 4-1

Peak water level in feet referenced to MLLW at San Francisco station (9414290) for 12 events derived from combining four peak astronomical tides with three peak residual tides

Peak Residual (Feet MLLW)	Peak Astronomical Tide (feet MLLW)			
	5.15	5.85	6.55	7.25
0.5	Event 1: 5.65	Event 4: 6.35	Event 7: 7.05	Event 10: 7.75
1.5	Event 2: 6.65	Event 5: 7.35	Event 8: 8.05	Event 11: 8.75
2.5	Event 3: 7.65	Event 6: 7.35	Event 9: 9.05	Event 12: 9.75

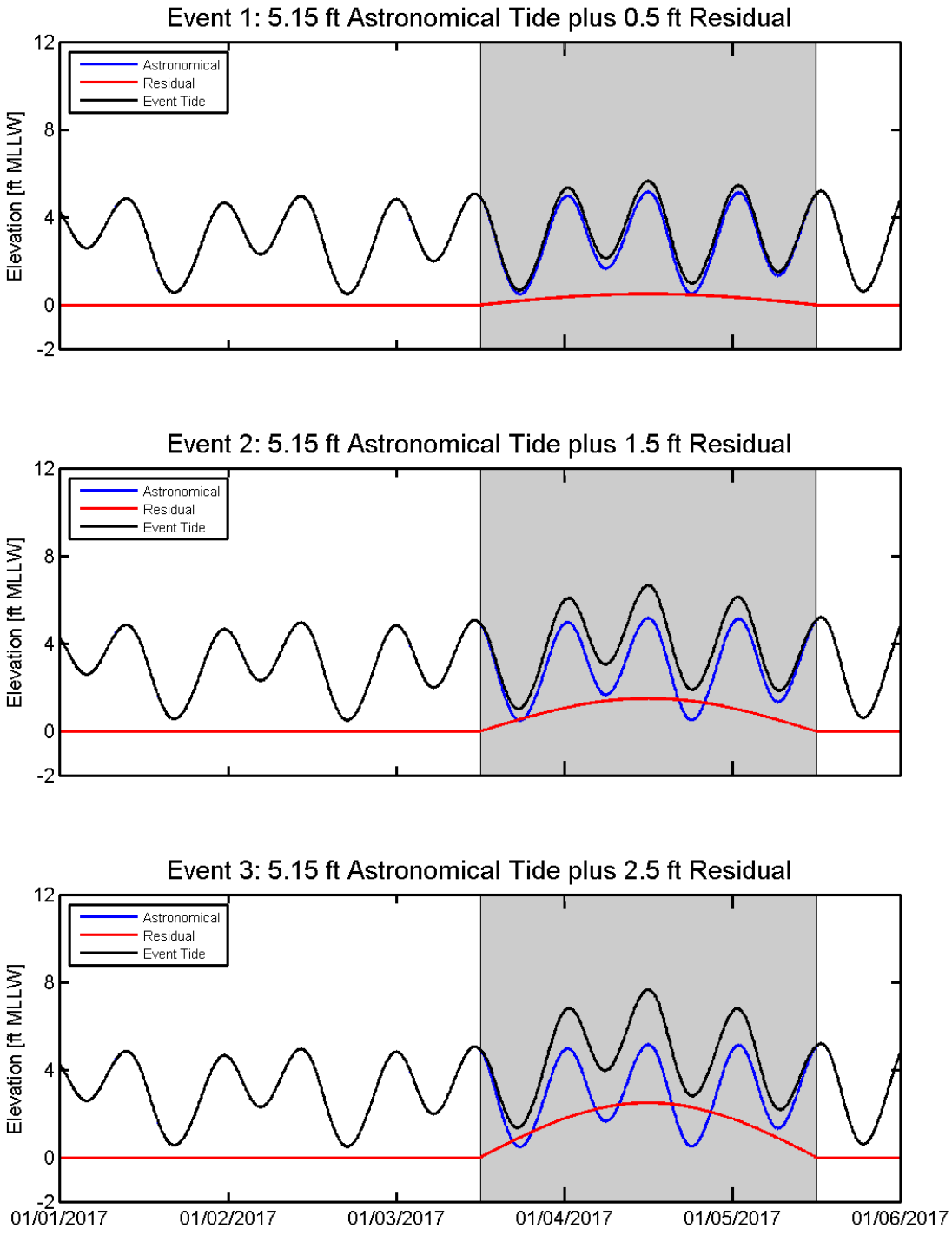

Figure 4.1-1

Astronomical tides generated from tidal harmonics, residual, and resulting event water surface elevations in feet referenced to MLLW at San Francisco for Event 1 through Event 3

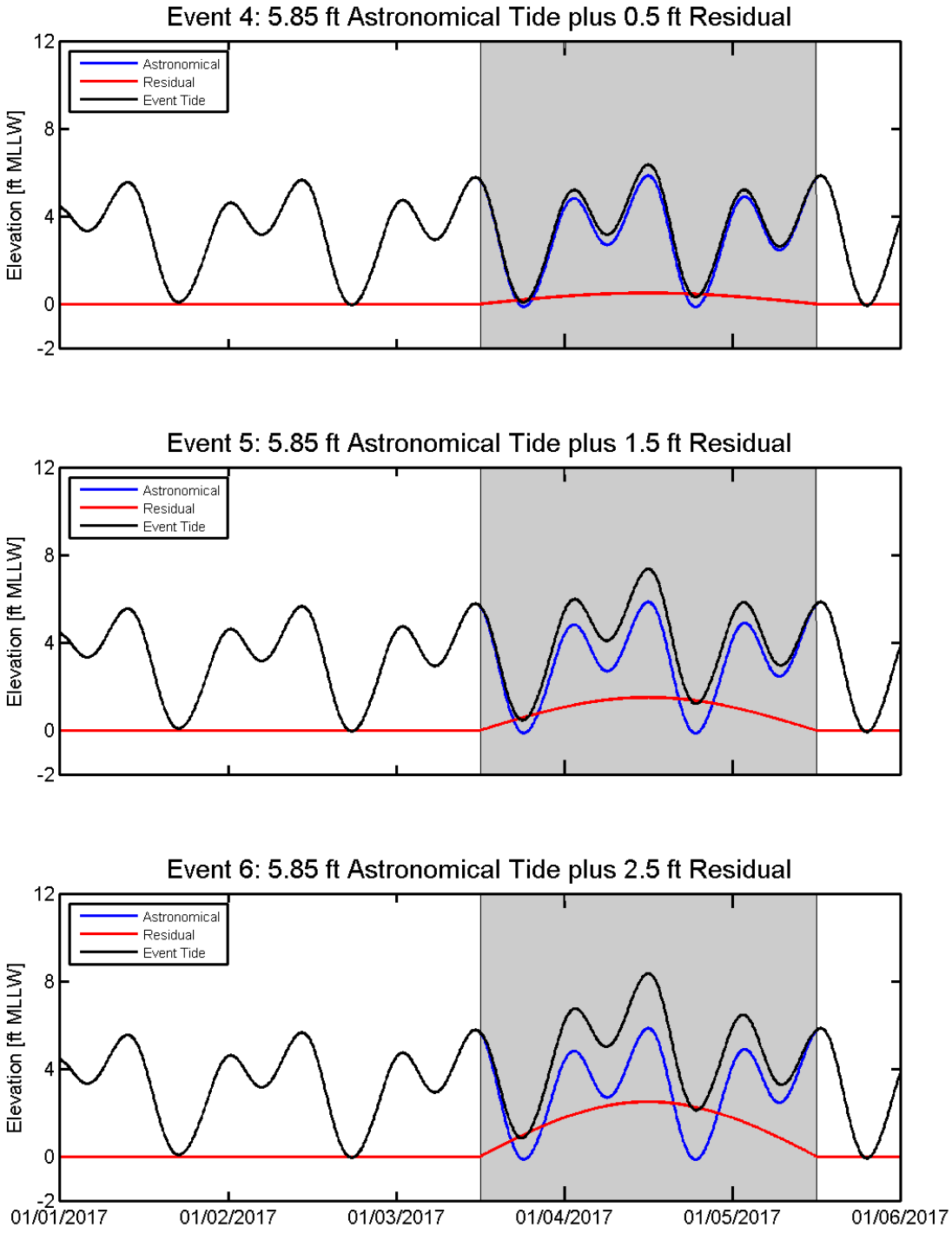

Figure 4.1-2

Astronomical tides generated from tidal harmonics, residual, and resulting event water surface elevations in feet referenced to MLLW at San Francisco for Event 4 through Event 6

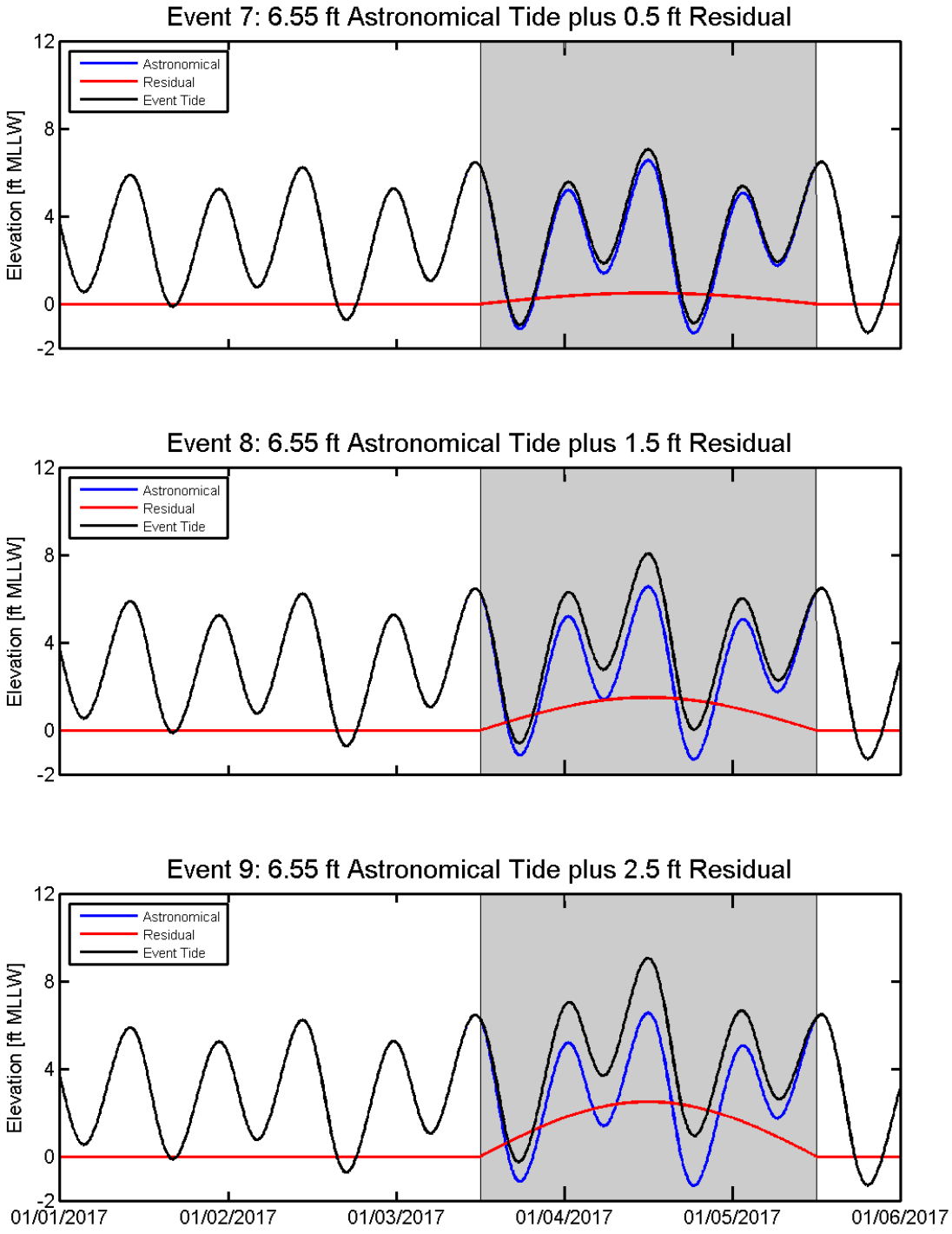

Figure 4.1-3

Astronomical tides generated from tidal harmonics, residual, and resulting event water surface elevations in feet referenced to MLLW at San Francisco for Event 7 through Event 9

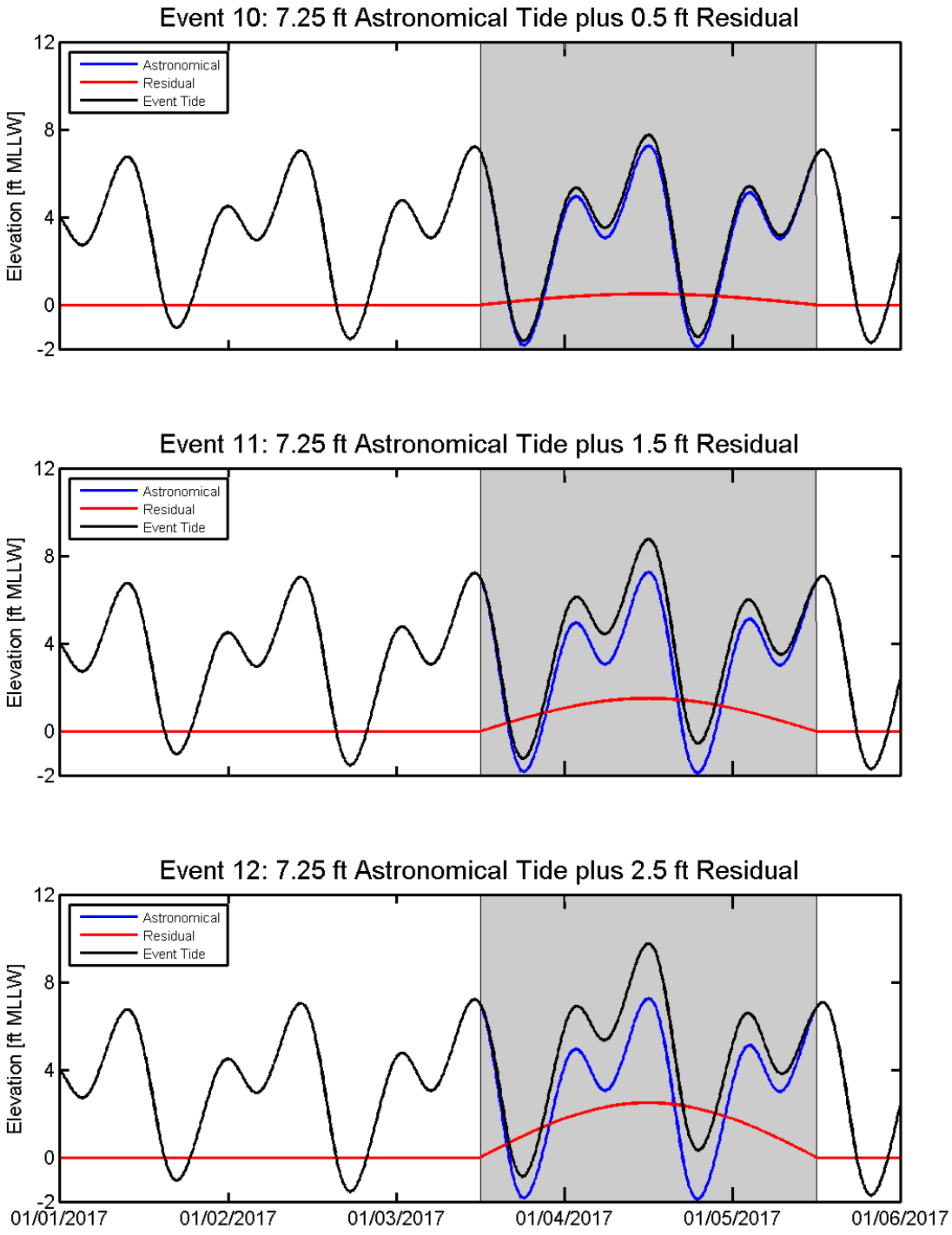

Figure 4.1-4

Astronomical tides generated from tidal harmonics, residual, and resulting event water surface elevations in feet referenced to MLLW at San Francisco for Event 10 through Event 12

4.2 River and Creek Inflow Boundary Conditions

The UnTRIM Bay-Delta model includes freshwater inflows from the Sacramento-San Joaquin Delta and tributaries which flow directly into San Francisco Bay. A sensitivity analysis by Letter and Sturm (2010) found that raising the Delta outflow from 11,000 cubic feet per second (cfs) to 300,000 cfs resulted in only a 0.03 foot increase in the peak residual water level at Coyote Creek, whereas the impact of increasing South Bay inflows from 278 cfs to 20,000 cfs raised the peak residual water level at the mouth of Coyote Creek by 0.16 foot. This suggests that peak water levels within the project area are likely to be sensitive to local tributary inflows but not sensitive to changes in inflows from the North Bay or the Delta.

The inflows to the UnTRIM Bay-Delta model were determined using the same methods as in the SSFBSS (MacWilliams et al. 2012). A constant inflow rate was used for all Year 0 and Year 50 scenario events for all river inflows with the exception of the twelve creek and river inflows south of Dumbarton Bridge. For all other model inflows, the average January flow was calculated for each Bay and Delta tributary and each export (see Figure 3.3-1) using available daily flow data for all days during January from 1980 to 2011. The resulting average January flows represent elevated flows typical of winter conditions, but not extreme flood peaks, and were applied as constant inflow rates for each of the scenarios.

The inflows for Coyote Creek and Guadalupe River were the same as those used in the SSFBSS (MacWilliams et al. 2012). For Coyote Creek and Guadalupe River, a relationship was developed between coastal residual and peak fluvial flow using historical flow data from the USGS and historic residual data observed at San Francisco (9414290). Figure 4.2-1 shows the correlation between peak fluvial flow measured on Guadalupe River and the coincident tidal residual observed at San Francisco (9414290). The linear trend line indicates that increasing peak fluvial flow correlates with increasing tidal residual. Figure 4.2-2 shows the correlation between peak fluvial flow measured on Coyote Creek and the coincident tidal residual observed at San Francisco (9414290). The linear trend line indicates that there is not a strong correlation on Coyote Creek between peak fluvial flow and tidal residual. The absence of a correlation may be due to the regulation of peak flows in Coyote Creek by upstream reservoirs (MacWilliams et al. 2012).

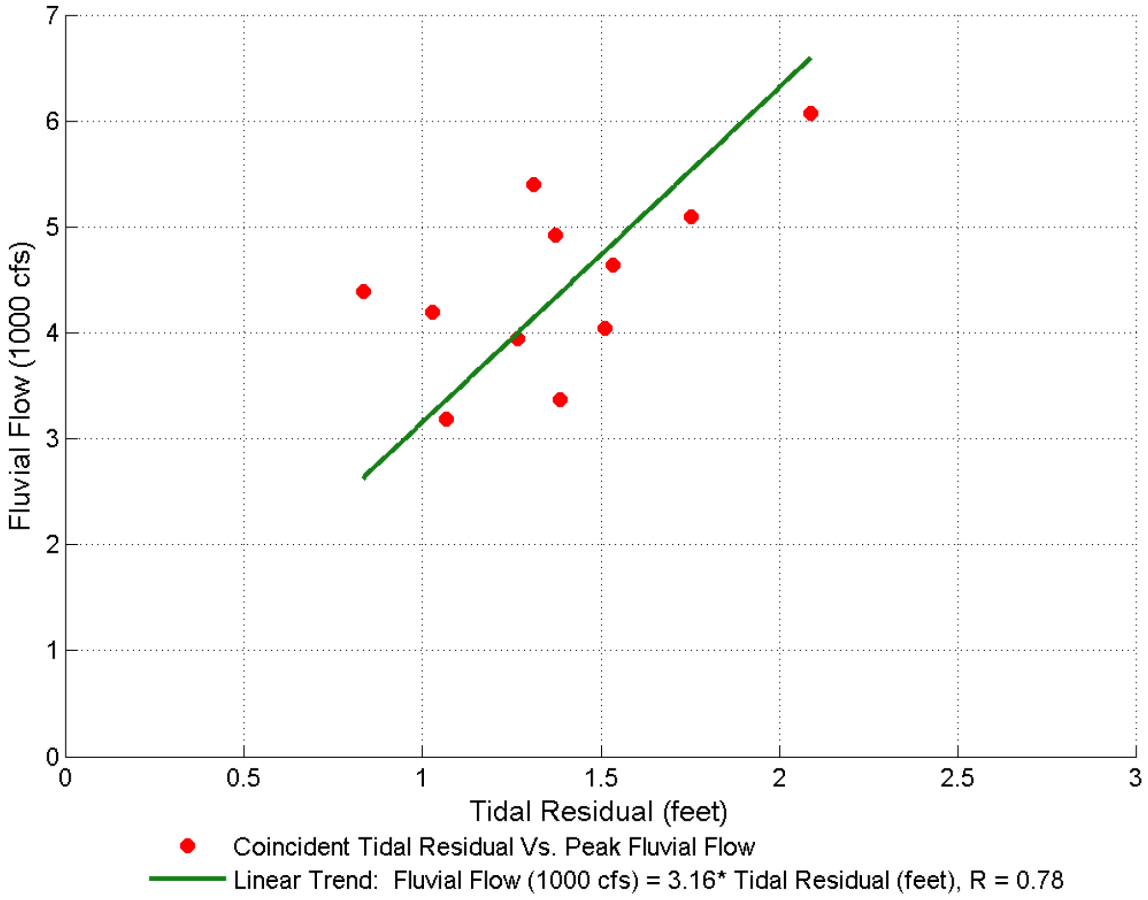

Figure 4.2-1
Relationship between peak fluvial flow and coincident tidal residual for Guadalupe River (from MacWilliams et al. 2012)

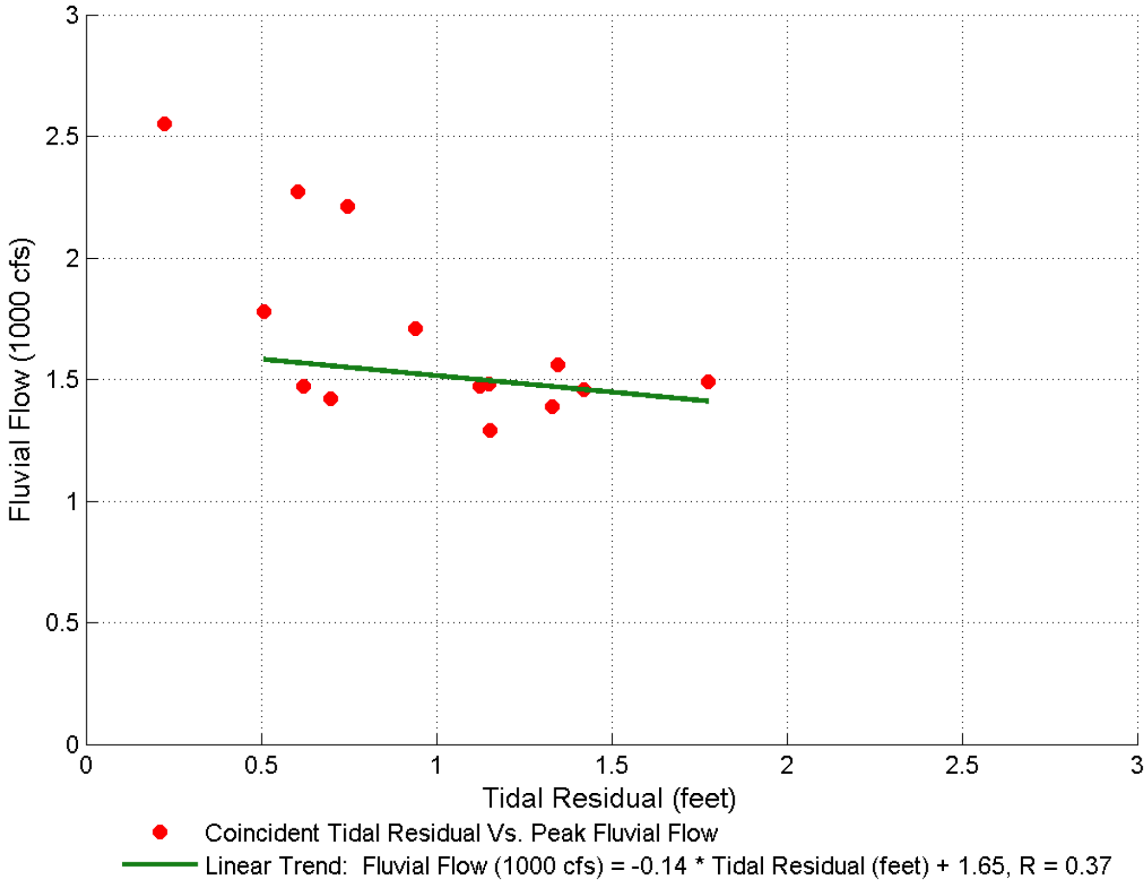

Figure 4.2-2
Relationship between peak fluvial flow and coincident tidal residual for Coyote Creek (from MacWilliams et al. 2012)

For Guadalupe River, the linear relationship shown on Figure 4.2-1 was used to develop three peak flow hydrographs based on the three peak residual events simulated. Based on an evaluation of historic flood hydrographs on Coyote Creek and Guadalupe River, most flow events last for about 12 hours (MacWilliams et al. 2012). On average, the peak flow on Guadalupe River occurred 5.7 hours after the peak residual tide at the San Francisco NOAA station (9414290), and the peak flow on Coyote Creek occurred 11.1 hours after the peak residual tide at the San Francisco NOAA station (9414290). As a result, the duration of each synthetic flow event on the Guadalupe River was assumed to be 12 hours, with the peak flow occurring 5.7 hours after peak residual. Prior to and subsequent to the peak flow event, the average January flow calculated for Guadalupe River was used. For Coyote Creek, the peak

flow was assumed to be identical for all events. The y-intercept value of 1,650 cfs (46.7 $m^3 s^{-1}$) from the linear fit, as shown on 4.2-2, was used as the peak flow on Coyote Creek for all events, with the peak flow occurring 11.1 hours after peak residual, and all events were assumed to last 12 hours. The shape of the hydrograph was developed based on a sine curve. Prior to and subsequent to the peak flow event, the average January flow calculated for Coyote Creek was used. The resulting inflow hydrographs used for Coyote Creek and Guadalupe River are shown in Figure 4.2-3.

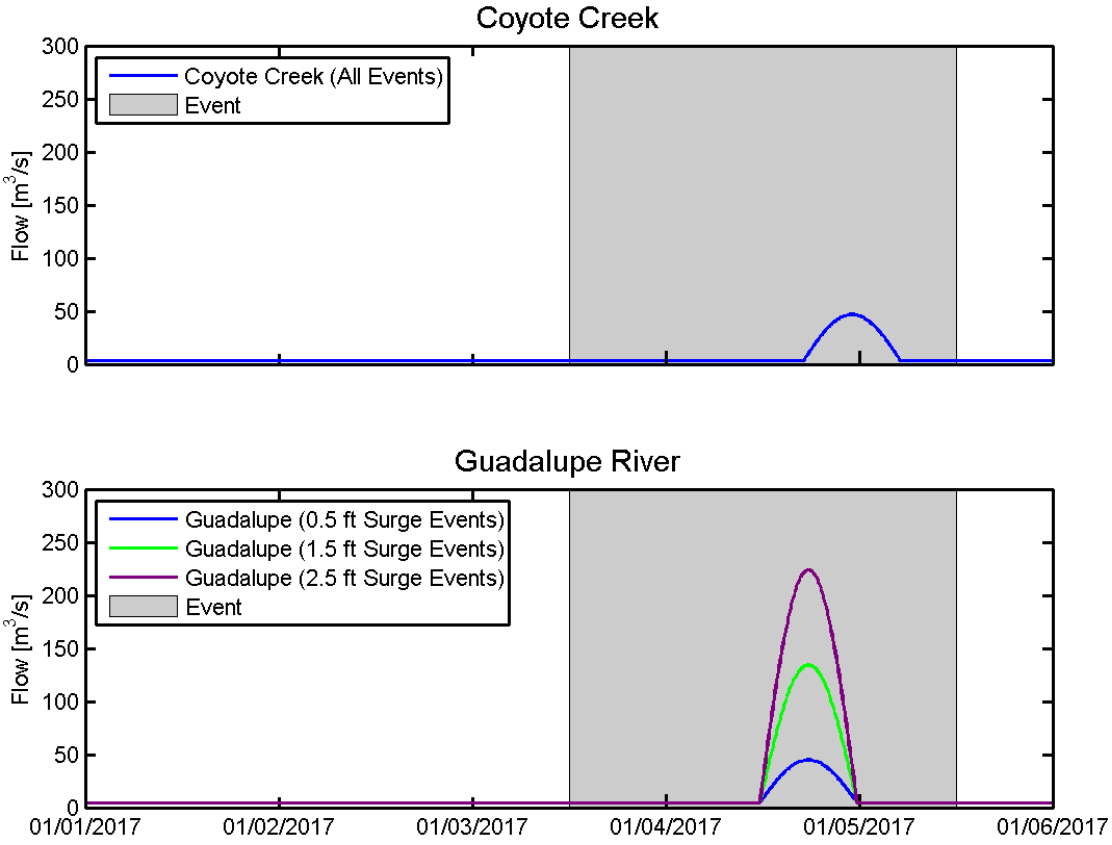

Figure 4.2-3
Inflow hydrograph for Coyote Creek (top) and Guadalupe River (bottom) used for Year 0 and Year 50 scenarios

Of the 10 inflows within the project area, only San Francisquito Creek and San Tomas Aquino Creek had sufficient data for determining the relationship between tidal residual and flow (USACE 2010). However, because the data for San Francisquito Creek contained no flow data for conditions near a residual of 2.5 ft, only the data from San Tomas Aquino Creek

were used to develop the relationship between residual and flow for this study. For San Tomas Aquino Creek, a relationship was developed between coastal residual and peak fluvial flow using historical flow data from the USGS and historic residual data observed at San Francisco (9414290). Figure 4.2-4 shows the correlation between peak fluvial flow measured on San Tomas Aquino Creek and the coincident tidal residual observed at San Francisco (9414290). The linear trend line indicates increasing peak fluvial flow correlates with increasing tidal residual. Based on this trend line, the flows on San Tomas Aquino Creek which were calculated to correspond to the tidal residuals of 0.5, 1.5, and 2.5 feet were 369 cfs, 2,616 cfs, and 4,863 cfs, respectively.

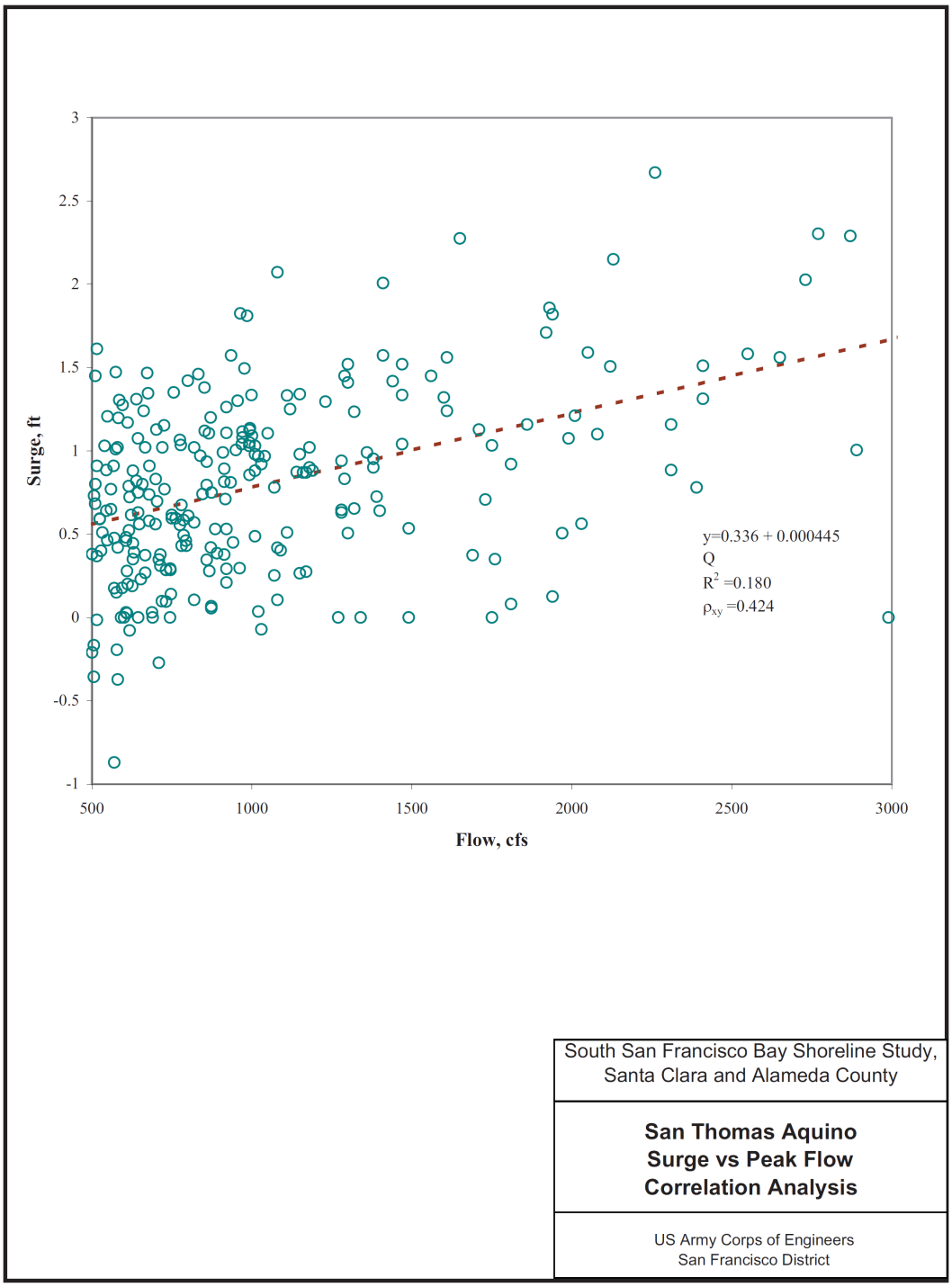

Figure 4.2-4

Relationship between peak fluvial flow and coincident tidal residual for San Tomas Aquino Creek (from USACE 2010)

Next, the 100-year flow was calculated for each of the 10 creeks within the project area, and the ratio of the 100-year flow on each individual creek relative to San Tomas Aquino creek was calculated (Table 4-2). As seen in Table 4-2, the 100-year flow on San Tomas Aquino Creek is greater than any of the three flow rates used for the three surge events. This results because the flows selected for this study were calculated to be coincident with storm surges of varying levels, and are therefore not necessarily 100-year flows. Because of this, it is important to recognize that along the creek portions of the model domain where water levels are dominated by fluvial, rather than coastal processes, the predicted maximum water levels cannot be used to calculate 100-year water levels, because all of the flows simulated are lower than 100-year flows, as is evident in a comparison of the 100-year flows (Table 4-2) and the simulated flows for each surge height (Table 4-3).

Table 4-2
100-year flows (cfs) for each creek in the project area and the ratio of each 100-year flow to San Tomas Aquino Creek (from Noble Consultants)

	San Francisquito	Matadero	Barron	Adobe	Permanente	Stevens	Sunnyvale W.	Sunnyvale E.	Calabazas	San Tomas Aq.
100-yr Flow	9,300	3,000	350	3,100	2,600	8,100	380	1,100	3,900	7,300
100-yr Ratio	1.27	0.41	0.05	0.42	0.36	1.11	0.05	0.15	0.53	1.00

Notes:
cfs = cubic feet per second
yr = year

The peak flows for each of the three residuals for San Tomas Aquino Creek (Table 4-3), which were calculated using the linear slope shown on Figure 4.2-4 (369 cfs, 2,616 cfs, and 4,863 cfs), were scaled to each of the remaining nine inflows in the study area based on the ratio of the 100-year flow in each tributary to the 100-year flow in San Tomas Aquino Creek (Table 4-2). The resulting peak inflows calculated for each surge height are shown in Table 4-3. The peak flow for San Francisquito Creek was capped at 4,000 cfs for the surge of 2.5 ft, because the existing creek levees along San Franciquito Creek overtop when flows exceed 4,000 cfs (Noble Consultants 2009). The use of a flow rate higher than 4,000 cfs would have precluded the possibility of distinguishing between flooding due to the creek levee

overtopping (which is not the focus of this study) or the project levee overtopping (which is the focus of this study).

Table 4-3

Peak flow (cfs) for each of the three residual (surge) events determined using the peak flow in San Tomas Aquino Creek and the 100 year flow ratios

Surge (feet)	Peak Flow (Scaled Based on San Tomas Aquino Creek)									
	San Francisquito	Matadero	Barron	Adobe	Perman-ente	Stevens	Sunnyv-ale W.	Sunnyv-ale E.	Cala-bazas	San Tomas Aq.
0.5	468	151	18	155	133	409	18	55	195	369
1.5	3,322	1,072	131	1,099	942	2,903	131	392	1,386	2,616
2.5	4,000	1,994	243	2,042	1,751	5,398	243	729	2,577	4,863

Note:
cfs = cubic feet per second

Based on an evaluation of historic flood hydrographs on Coyote Creek and Guadalupe River, most flow events last for about 12 hours (MacWilliams et al. 2012). On average, the peak water level at the western extent of Coyote Creek near the study region occurred 1.5 hours after the peak water level at the San Francisco NOAA station (9414290). As a result, the duration of each synthetic flow event on the ten creeks in the project area was assumed to be 12 hours, with the peak flow 1.5 hours after peak residual at the San Francisco NOAA station (9414290). Prior to and subsequent to the peak flow event, the base flow in each of the ten creeks was used as the inflow. Data was available for the base flow for San Francisquito Creek, Matadero Creek, Guadalupe River, and Coyote Creek (MacWilliams et al. 2012). The relationship between the base flows and the 100-year flows for these four inflows was used to determine the base flow for the eight remaining creeks in the project area. The base flow divided by the 100-year flow for the four inflows with base flow data ranged from 0.005 to 0.01. The base flows for the eight remaining creeks in the project area were set as 1% of the 100 year flow. The resulting hydrographs for the ten creeks within the study area are shown on Figure 4.2-5 and Figure 4.2-6.

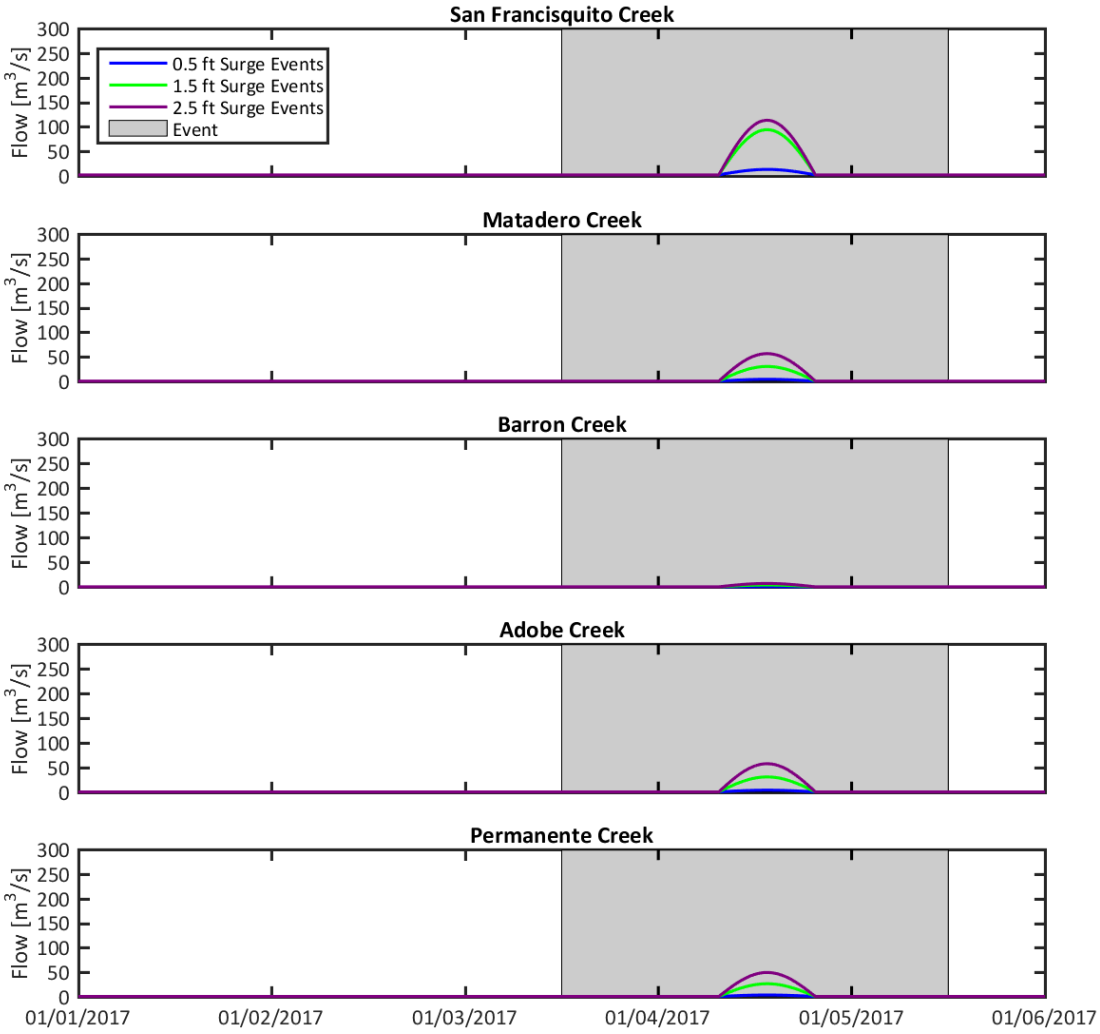

Figure 4.2-5

Inflow hydrograph for San Francisquito Creek, Matadero Creek, Barron Creek, Adobe Creek, and Permanente Creek used for Year 0 and Year 50 scenarios

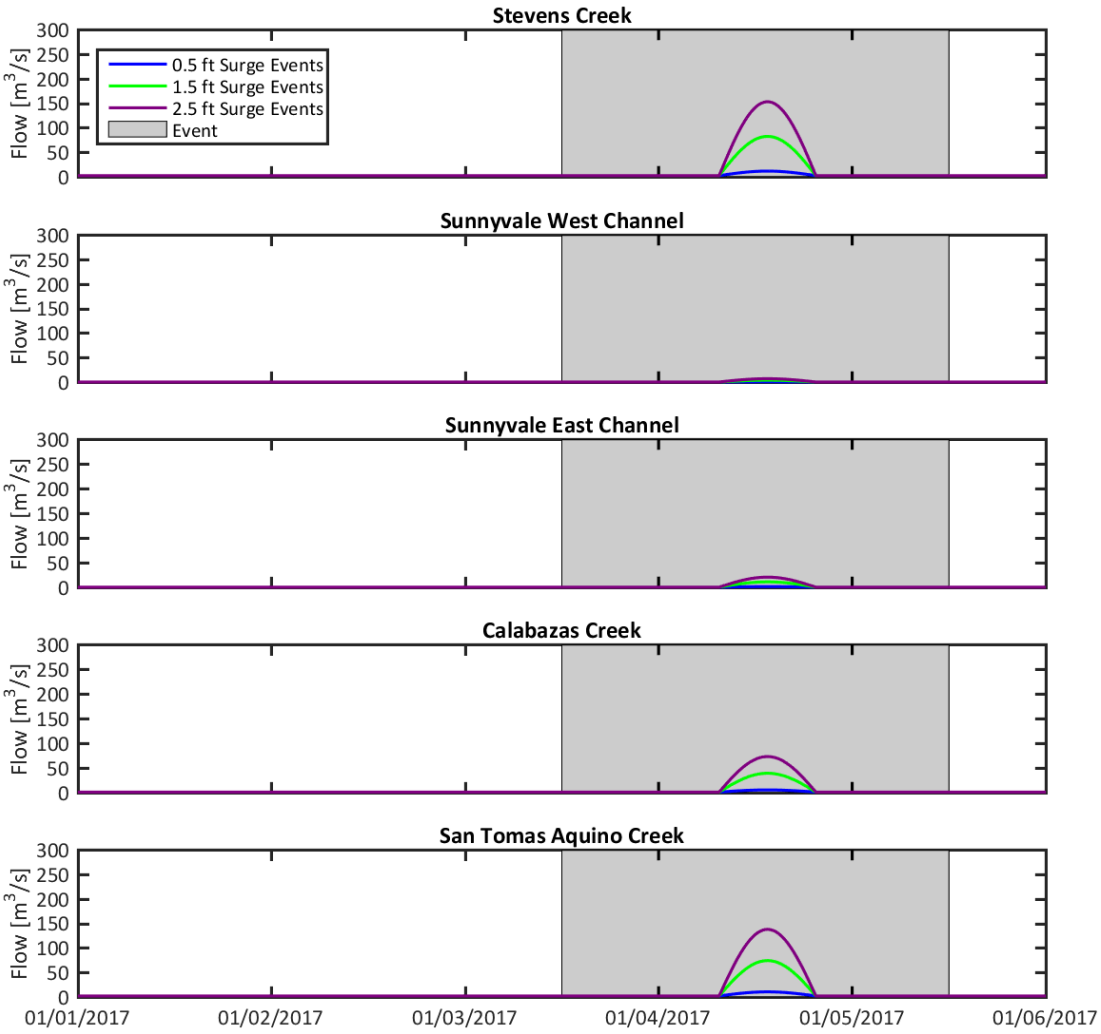

Figure 4.2-6

Inflow hydrograph for Stevens Creek, Sunnyvale West Channel, Sunnyvale East Channel, Calabazas Creek, and San Tomas Aquino Creek used for Year 0 and Year 50 scenarios

4.3 Wind Boundary Conditions

A set of synthetic wind events were developed to represent the range of potential wind conditions that are likely to result in significant wind induced setup in the project area. Wind can result in a significant increase in the maximum predicted water level in the project area during periods with relatively strong winds aligned with the axis of South San Francisco Bay (MacWilliams et al. 2012). Conversely, during a period of weaker winds from the south, wind can result in a decrease in water levels in the south end of South San Francisco Bay.

Based on an analysis of historic wind data at San Francisco International Airport, the most frequently occurring wind directions which lead to significant wind setup in the South Bay are 292.5 and 315 degrees (MacWilliams et al. 2012). These two wind directions are approximately aligned with the axis of South San Francisco Bay. Analysis of wind events in San Francisco Bay suggests a typical duration of approximately 20 hours (MacWilliams et al. 2012). For the six synthetic wind events, three non-zero wind speeds with two wind directions were simulated, as shown in Table 4-4. Figure 4.3-1 shows the wind speed and direction spanning the five day simulation period for the six wind events. In each wind event, the wind speed ramps up for 2 hours, remains constant for 16 hours, and ramps down for 2 hours. It is assumed the wind event is coincident with the residual event such that the peak winds occur 8 hours before and after peak residual.

Six different wind conditions (Table 4-4) were simulated to evaluate wind setup for Event 1, Event 3, Event 10, and Event 12 (Table 4-1). The wind setup for each of the six non-zero wind scenarios were simulated for each of these four tidal events, and the wind setup for each wind scenario was calculated as the difference between the peak water surface elevation from the simulation with wind and the peak water surface elevation from the corresponding simulation without wind. This approach assumes the wind setup can be decoupled from the residual events and allows for 2-D interpolation of wind effects based on residual and stage in the Monte Carlo simulation analysis.

Table 4-4

Synthetic wind events used in the scenarios to develop wind setup lookup tables

Wind Direction (degrees)	Maximum Sustained Wind Speed (mph)			
	0 mph	20 mph	30 mph	40 mph
292.5	0 mph from 292.5 degrees	20 mph from 292.5 degrees	30 mph from 292.5 degrees	40 mph from 292.5 degrees
315.0	0 mph from 315.0 degrees	20 mph from 315.0 degrees	30 mph from 315.0 degrees	40 mph from 315.0 degrees

Note:
mph = miles per hour

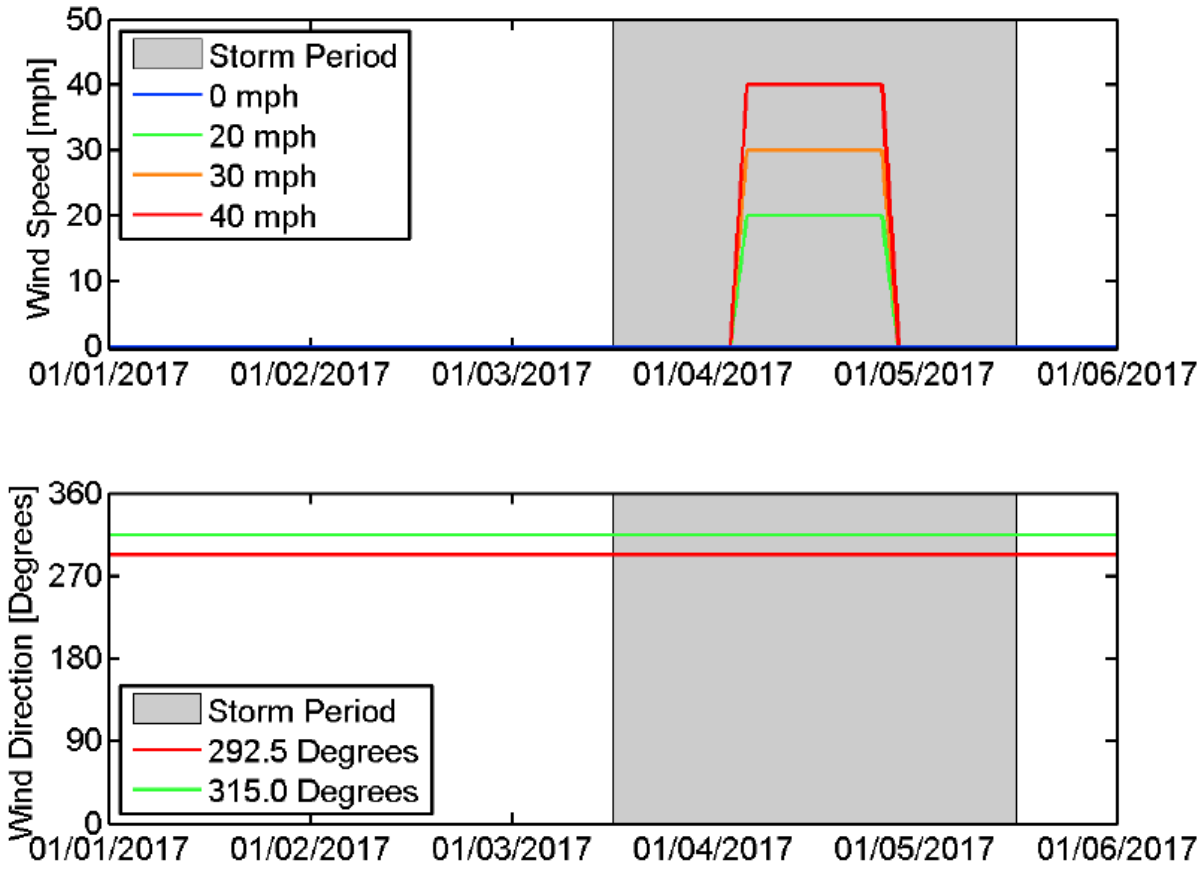

Figure 4.3-1
Predicted wind speed for four maximum sustained wind speeds (top) and wind direction for two wind directions (bottom) used in the scenarios to develop wind lookup tables

4.4 Sea Level Rise Assumptions

Sea level rise (SLR) projections developed for this study are based on procedures prescribed by ER 1100-2-8162 (USACE 2013). The geographically closest suitable NOAA tide gage to the project area is the NOAA San Francisco tide gage (9414290). USACE guidance calls for projecting SLR change from the midpoint of the National Tidal Datum Epoch (NTDE), which is 1992 (USACE 2014).

For the Year 0 conditions in 2017, SLR was calculated between 1992 and 2017 using the USACE Low Curve, which is based on the historic rate of sea level change. The USACE Low Curve estimated 0.17 ft (0.0518 meters [m]) of SLR between 1992 and 2017. Thus, for all Year 0 scenarios, the ocean boundary condition was adjusted upward to result in 0.17 ft of

SLR at the San Francisco NOAA tide station for each simulation to account for SLR that occurred between the midpoint of the NTDE (1992) and 2017.

For the Year 50 conditions in 2067, SLR was calculated between 2017 and 2067 using the USACE Low Curve, which is based on the historic rate of sea level change, the USACE Intermediate Curve, which is computed from the modified National Research Council (NRC) Curve I, considering both the most recent Intergovernmental Panel on Climate Change (IPCC) projections and modified NRC projections with the local rate of vertical land movement added, and the USACE High Curve which is computed from the modified NRC Curve III, considering both the most recent IPCC projections and modified NRC projections with the local rate of vertical land movement added. Based on these projections, the Year 50 scenarios were designed by adjusting relative sea level upward by 0.51 ft between 1992 and 2067 for the USACE Low Curve, 1.01 ft between 1992 and 2067 for the USACE Intermediate Curve, and 2.59 ft between 1992 and 2067 for the USACE High Curve.

4.5 Additional Boundary Conditions and Assumptions

For each set of scenarios for Year 0 existing conditions (Section 5.1), Year 50 existing conditions (Section 5.2), Year 0 with-project conditions (Section 6.1), and Year 50 with-project conditions (Section 6.2), additional boundary conditions were required to account for salt pond operations, initial water levels in the salt ponds, restoration assumptions for the salt ponds, morphological change and accretion within restored ponds for future conditions, and the number and locations of levee breaches. Because these boundary conditions and assumptions varied between each set of conditions, the details of the boundary condition assumptions specific to each of these sets of scenarios is discussed in Sections 5 and 6.

5 SIMULATION OF EXISTING CONDITIONS FOR YEAR 0 AND YEAR 50

This section provides a description of the modeling assumptions and boundary conditions for the existing conditions scenarios. A total of 720 scenarios were developed to span the range of boundary conditions and levee breaches for existing conditions for Year 0 and Year 50.

5.1 Scenario Matrix and Modeling Assumptions for Year 0 Existing Conditions Simulations

5.1.1 Description of Year 0 Existing Conditions Scenarios

A total of 180 scenarios were conducted for Year 0 under existing conditions. These scenarios were developed using the 12 water level and flow events, six wind combinations, and five breach zones (Table 5-1). The first set of 36 scenarios consists of 12 scenarios representing the combined tide and surge for Events 1 through 12 (Table 4-1) with no wind. The remaining 24 of the 36 scenarios were designed to determine the contribution of wind to the peak water surface elevation for a range of wind speeds and directions. These 24 scenarios use the tidal forcing for four events (1, 3, 10, and 12) with six different combinations of wind speed and direction (Table 4-4). The combination of no-wind and with-wind scenarios results in a total of 36 scenarios for Year 0 existing conditions, with no inner or outer levee breaches.

Table 5-1
Year 0 Existing Conditions Scenarios

Without-Project Scenario	Year	SLR Rate	Inner Breaches	Outer Breaches	Number of Scenarios
Existing Levee	0	None	None	None	36
			EIA 1 to EIA 3	EIA 1 to EIA 3	36
			EIA 4 & EIA 5	EIA 4 & EIA 5	36
			EIA 6 & EIA 7	EIA 6 & EIA 7	36
			EIA 8 & EIA 9	EIA 8 & EIA 9	36
			EIA 10	EIA 10	0
Total Number of Year 0 Existing Conditions Scenarios					**180**

Notes:
EIA = Economic Interest Area
SLR = sea level rise

In order to provide water surface elevations for scenarios in which the levees were assumed to fail during the Monte Carlo simulation analysis, additional scenarios were simulated that included inner and outer levee failures. Although it is not known in advance exactly where levee failures will occur, it was necessary to assume specific breach locations in order to conduct the breach scenarios. Levee breach locations were chosen to occur near locations where the current levees may naturally overtop during periods of very high water surface elevation (Figure 5.1-1). The breach invert for each levee failure was determined based on the approximate elevation of the inner toe of the levee at each breach location.

Due to the large combined area of EIA 1 through EIA 10, the scenarios with levee breaches used five separate breach zones, because assuming that all breaches occur together could lead to an under prediction of peak water levels. Breach Zone 1 included EIA 1 through 3, Breach Zone 2 included EIA 4 and 5, Breach Zone 3 included EIA 6 and 7, Breach Zone 4 included EIA 8 and 9, and Breach Zone 5 included EIA 10 (Table 5-1). Because the focus of this study is the coastal levee only, no creek levees were breached in any of the scenarios, resulting in no levee breaches into EIA 3 because it is not adjacent to the project levee and is separated from the project levee by creek levees. The portion of EIA 10 between Calabazas Creek and San Tomas Aquino Creek near the project levee is very high in elevation, and as a result, no levee breach scenarios were conducted for EIA 10.

For each breach zone, a total of 36 scenarios were simulated to develop lookup tables for water levels both bayward and landward of the levees in the event that the inner and outer levees failed. These 36 scenarios used the same combinations of tidal events and wind conditions as described for the 36 no-breach scenarios. All breach scenarios under existing conditions assumed that both the outer and inner levees within a breach zone are breached at the same time. Inner breaches are breaches of the project levee or behind the project levee, while outer breaches are breaches in the salt pond levees on the bayward side of the project levee.

Figure 5.1-1
Levee breach locations for each breach zone for Year 0 and Year 50 existing conditions scenarios. Black lines are creek and pond levees and the green line shows the model grid extent.

5.1.2 Salt Pond Operations and Water Surface Elevations for Year 0 Existing Conditions Scenarios

The Year 0 existing conditions scenarios assume that the salt ponds are operated similarly to how they are currently operated during winter, and that further restoration of these ponds has not yet begun in Year 0. The operations of the salt ponds seaward of EIA 1 through EIA 11 were developed based on typical winter operating conditions (Figure 5.1-2). The initial water surface elevations in the salt ponds were also based on typical winter operating levels (Schaaf & Wheeler 2005) and updated to be consistent with available information on current winter operations (E. Mruz and J. Bourgeois 2014).

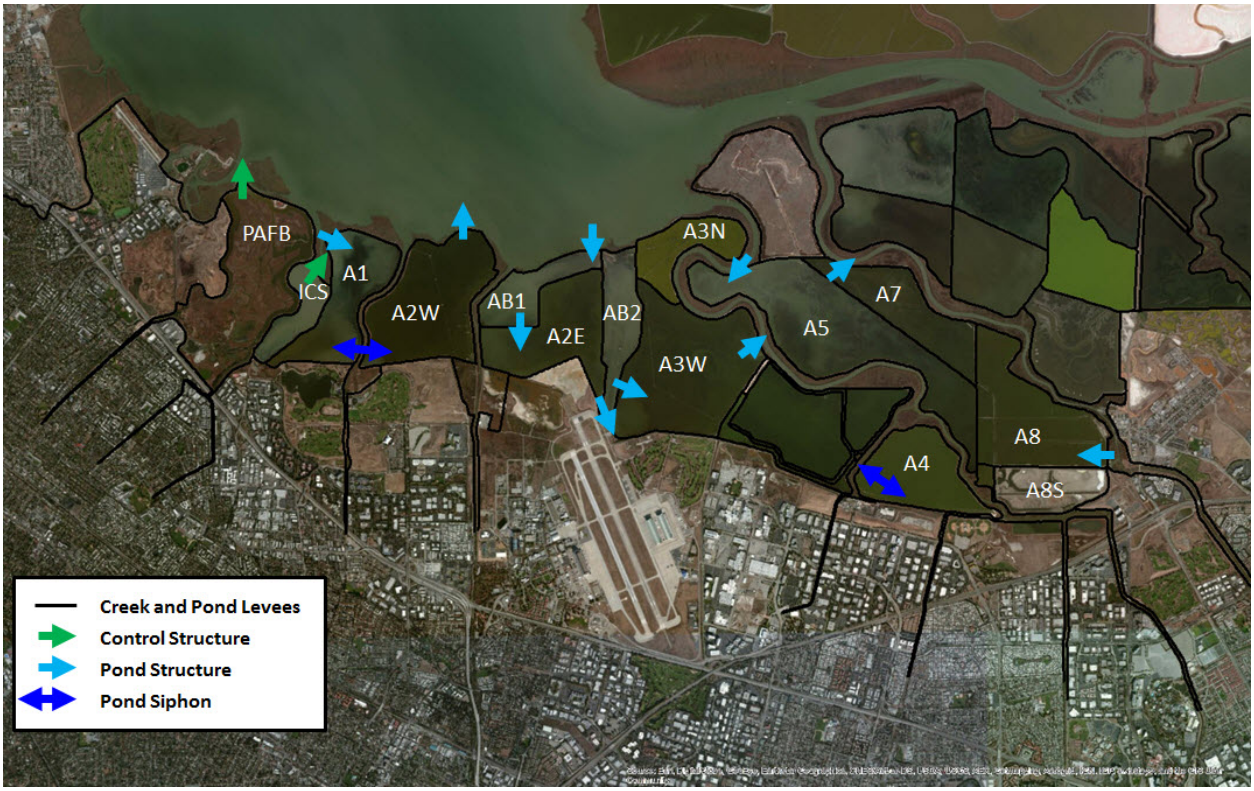

Figure 5.1-2
Locations of control structures and siphons for the Palo Alto Flood Basin (PAFB), Inner Charleston Slough (ICS), and Ponds A1 through A8, which are bayward of EIAs 1 through 10 under existing conditions

5.1.2.1 Palo Alto Flood Basin and Inner Charleston Slough

The Palo Alto Flood Basin (PAFB) was created in 1956 with the construction of levees surrounding a 600-acre portion of the Palo Alto Baylands (Schaaf & Wheeler 2014). The PAFB receives inflow from Matadero Creek, Adobe Creek, and Barron Creek. The tide gate structure that allows flow between the PAFB and South San Francisco Bay consists of 8 box culverts, each with two 5-foot by 5-foot flap gates on the downstream face. The tide gates have an invert elevation of approximately -3.0 feet NAVD88. The flap gates open when the water elevation in the PAFB is higher than the San Francisco Bay tide elevation. Although the City of Palo Alto opens one of the tide gates during summer months to allow circulation of brackish Bay water within the PAFB, under winter operating conditions, the gates close when San Francisco Bay tides rise above the elevation of stored water in the PAFB to prevent Bay waters from entering the PAFB, thereby maintaining available volume for holding creek

runoff during high flow events. The Year 0 existing conditions scenarios assume the gates are operated under winter conditions and allow outflow only, and the initial water level inside the PAFB is assumed to be 0.5 ft NAVD88. However, because the water levels inside PAFB are controlled by inflow from Matadero Creek, Adobe Creek, Barron Creek and the capacity of the outlet structure to release flow at low water, the water surface elevations inside the PAFB predicted in this analysis should not be considered 100-year water levels inside the PAFB because the inflows to PAFB in the scenario simulations are considerably lower than 100-year flows (Tables 4-2 and 4-3). As a result, the primary objective of including PAFB operations in these scenarios is to accurately predict water levels on the bayward side of the PAFB levee due to coastal flooding.

Inner Charleston Slough (ICS) is connected to South San Francisco Bay by a structure consisting of six culverts with self-closing tide gates that close when water levels on the Bay side of the structure are high to maintain the freeboard requirements, resulting in muted tidal fluctuations within ICS (Hydroikos 2009). Based on typical operations for February 2009 (Hydroikos 2009), the structure is operated to maintain maximum water levels of around 4.7 ft NAVD88. As a result, an initial water level of 4.7 ft NAVD88 was assumed inside ICS and the tide gates were operated to close when the water levels outside ICS exceeded 4.7 ft NAVD88.

5.1.2.2 Ponds A1 and A2W

The pond operations for Pond A1 and A2W under Year 0 existing conditions assume a single 48-inch inlet gate to Pond A1 from Charleston Slough, a 72-inch siphon under Mountain View Slough between Pond A1 and A2W, and a single 48-inch outlet gate to the Bay from Pond A2W (Figure 5.1-2). The initial water level inside both Pond A1 and Pond A2W is assumed to be 2.1 ft NAVD88.

5.1.2.3 Ponds AB1 to A3W

The pond operations for Pond AB1 under Year 0 existing conditions assume one 48-inch and one 36-inch inlet gate from the Bay to Pond AB1. There is an existing gap between Pond AB1 and AB2, and it is assumed no changes are made to the existing connections between Pond A3N and Ponds A3W and AB2. A 48-inch gate allows flow from Pond AB1 to Pond

A2E. A series of two 36-inch pipes connect Pond A2E to Pond A3W, and a single 36-inch gate connects Pond AB2 to Pond A3W. The outlet structure from Pond A3W to Guadalupe Slough consists of three 48-inch pipes, which, under winter operating conditions, only allow unidirectional flow from A3W to Guadalupe Slough. The initial water level inside Pond AB1 and Pond AB2 is assumed to be 3.6 ft NAVD88. The initial water level inside Pond A2E and Pond A3W is assumed to be 0.9 ft NAVD88. Pond A3N is assumed to operate seasonally and is assumed to be initially dry.

5.1.2.4 Pond A4

Under existing conditions, there is a 72-inch siphon between Pond A4 and the east end of the Cargill channel (Figure 5.1-2). At the western end of the Cargill channel, there is an opening that allows flow between Pond A3W and the Cargill channel. Through these connections, water levels in Pond A4 are effectively controlled by water levels in Pond A3W. The initial water level inside Pond A4 is assumed to be 0.9 ft NAVD88, which is identical to the initial water level assumed inside Pond A3W.

5.1.2.5 Ponds A5 to A8

The pond operations for Pond A5 and A7 under Year 0 existing conditions assume two 48-inch inlet gates to Pond A5 from Guadalupe Slough, existing gaps in the levee between Pond A5 and A7, and two 48-inch outlet gates from Pond A7 to Guadalupe Slough (Figure 5.1-2). The initial water level inside both Pond A5 and Pond A7 is assumed to be 3.1 ft NAVD88. Water levels inside Pond A8 are controlled by a single control structure that connects Pond A8 to Alviso Slough. This structure consists of a 40-foot armored notch with multiple bays that can be opened and closed independently (USFWS 2015). The Year 0 operating assumptions for this structure indicate 4 bays with a total width of 20 feet are open to Alviso Slough. Several openings in the historical levee between Pond A8 and Pond A8S allow for flow between these ponds.

5.1.2.6 Ponds A9 to A18

The Year 0 operating assumptions for Ponds A9 through A15 are identical to those used for the SSFBSS (MacWilliams et al. 2012). Year 0 operations for Ponds A16 and A17 are assumed to remain identical to current operations, with a single breach between A17 and Coyote

Creek, a control structure that allows flow from Pond A17 to A16, and an outlet control structure from Pond A16 to Artesian Slough. The Year 0 operating assumptions for Pond A18 are identical to those used for the SSFBSS (MacWilliams et al. 2012).

5.2 Scenario Matrix and Modeling Assumptions for Year 50 Existing Conditions Simulations

5.2.1 Description of Year 50 Existing Conditions Scenarios

Simulations were conducted to determine the peak water levels 50 years after the project study year of 2017, assuming existing levee and pond conditions. A total of 540 scenarios were conducted for Year 50 with existing levee conditions.

For Year 50 conditions, SLR was calculated between 2017 and 2067 using the USACE Low Curve, the USACE Intermediate Curve, and the USACE High Curve as described in Section 4.4. Based on these projections, the Year 50 scenarios were designed by adjusting relative sea level upward by 0.51 ft between 1992 and 2067 for the USACE Low Curve, 1.01 ft between 1992 and 2067 for the USACE Intermediate Curve, and 2.59 ft between 1992 and 2067 for the USACE High Curve. The Year 50 existing conditions scenarios include a full set of 180 scenarios for each of the three different SLR curves described in Section 4.4. The creek inflows, wind, and levee breach locations for Year 50 existing conditions were identical to those used for the Year 0 existing conditions scenarios.

For each SLR curve, the scenarios were developed using 12 water level and flow events, 6 wind combinations, and 5 breach zones (Table 5-2). For each SLR curve, the first set of 36 scenarios consists of 12 scenarios representing the combined tide and surge for Events 1 through 12 (Table 4-1) with no wind. The remaining 24 of the 36 scenarios for each SLR curve were designed to determine the contribution of wind to the peak water surface elevation for a range of wind speeds and directions. These 24 scenarios use the tidal forcing for four events (1, 3, 10, and 12) with 6 different combinations of wind speed and direction (Table 4-4). For each SLR curve, the combination of no-wind and with-wind scenarios results in a total of 36 scenarios for Year 50 existing conditions, with no inner or outer levee breaches.

The Year 50 existing conditions scenarios included the possibility of inner and outer levee failures at the same locations at which levee failures were considered under the Year 0 existing conditions (Figure 5.1-1). For each breach zone, a total of 36 scenarios were simulated for each SLR rate which included levee failures to develop lookup tables for water levels both bayward and landward of the levees in the event that the inner and outer levees failed. This resulted in a total of 144 scenarios which included levee breaches for each SLR curve (Table 5-2).

Table 5-2
Year 50 Existing Conditions Scenarios

Without-Project Scenario	Year	SLR Rate	Inner Breaches	Outer Breaches	Number of Scenarios
Existing Levee	50	USACE Low Curve	None	None	36
			EIA 1 to EIA 3	EIA 1 to EIA 3	36
			EIA 4 & EIA 5	EIA 4 & EIA 5	36
			EIA 6 & EIA 7	EIA 6 & EIA 7	36
			EIA 8 & EIA 9	EIA 8 & EIA 9	36
			EIA 10	EIA 10	0
Existing Levee	50	USACE Intermediate Curve	None	None	36
			EIA 1 to EIA 3	EIA 1 to EIA 3	36
			EIA 4 & EIA 5	EIA 4 & EIA 5	36
			EIA 6 & EIA 7	EIA 6 & EIA 7	36
			EIA 8 & EIA 9	EIA 8 & EIA 9	36
			EIA 10	EIA 10	0
Existing Levee	50	USACE High Curve	None	None	36
			EIA 1 to EIA 3	EIA 1 to EIA 3	36
			EIA 4 & EIA 5	EIA 4 & EIA 5	36
			EIA 6 & EIA 7	EIA 6 & EIA 7	36
			EIA 8 & EIA 9	EIA 8 & EIA 9	36
			EIA 10	EIA 10	0
Total Number of Year 50 Existing Conditions Scenarios					**540**

Notes:
EIA = Economic Interest Area
SLR = sea level rise
USACE = U.S. Army Corps of Engineers

5.2.2 Year 50 Bathymetry for Existing Conditions

The projection of bathymetry for 2067 within the project area is subject to significant uncertainty resulting from future weather and climate conditions, changes to the available sediment supply, SLR, the timing and design of the restoration of the former salt ponds to tidal action (including both the ponds in the project area and the adjacent ponds being restored as part of the South Bay Salt Pond Restoration Project), and the subsequent morphologic evolution of the restored ponds. As part of the SSFBSS (MacWilliams et al. 2012), a detailed analysis was conducted to develop the Year 50 bathymetry based on an analysis of recent historic bathymetric change, a projection of areas within the project area most likely to remain accretional under future conditions with SLR, and analysis of the potential for channel scour resulting from increased tidal prism from the restored pond areas. For this study, the accretion and scour projected for Year 50 existing conditions south of the Dumbarton Bridge as part of the SSFBSS (Figure 5.2-1) were applied for all Year 50 scenarios.

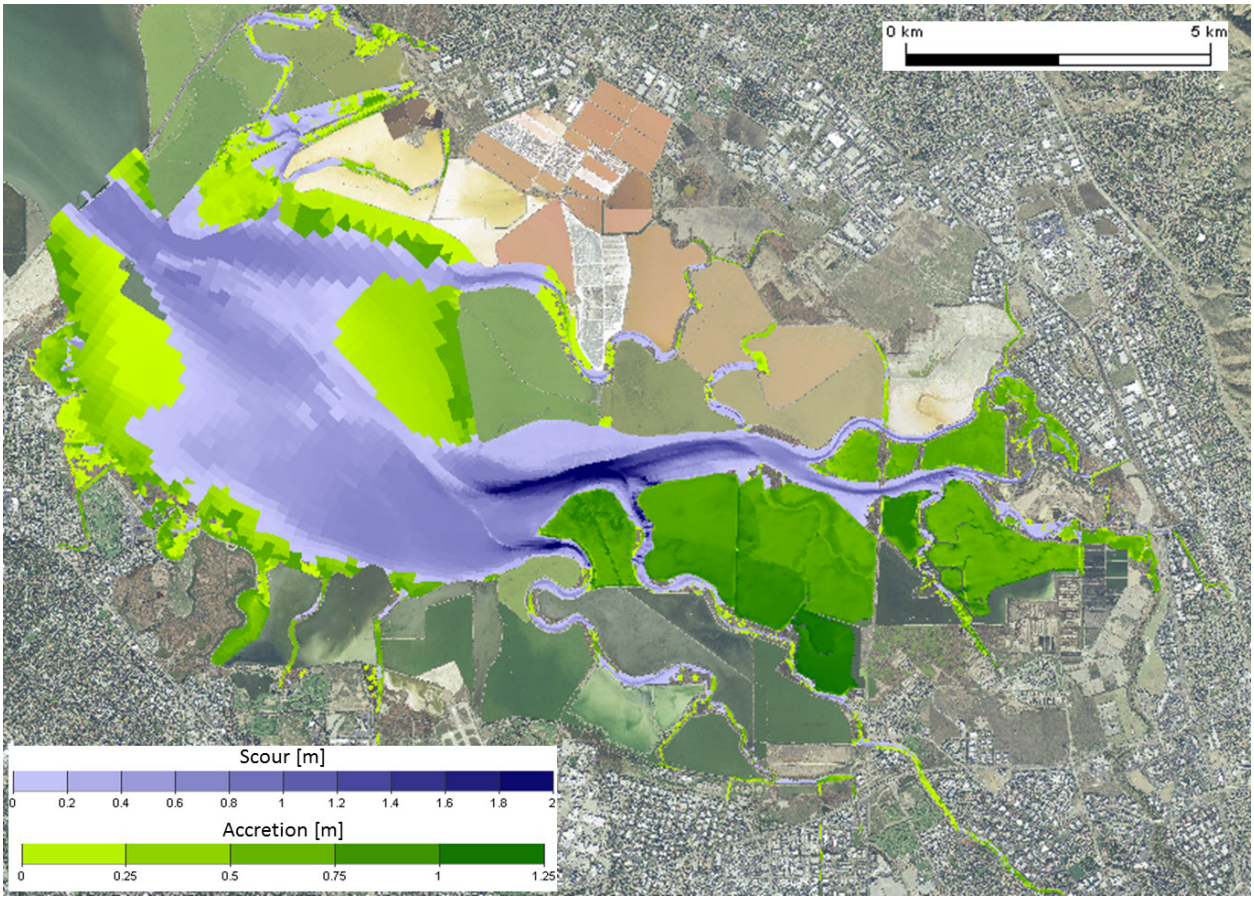

Figure 5.2-1
Predicted bathymetric change south of Dumbarton Bridge for Year 50 (2067) scenarios relative to 2010 conditions (from MacWilliams et al. 2012)

5.2.3 Salt Pond Operations and Water Surface Elevations for Year 50 Existing Conditions Scenarios

The Year 50 existing conditions scenarios assume no changes in the salt pond operations adjacent to EIA 1 through EIA 10 between Year 0 and Year 50, and the assumptions for the operations of PAFB, ICS, and Ponds A1 through A8 are identical to those described for Year 0 existing conditions in Section 5.1.2. It is assumed that under Year 50 conditions, the project levee adjacent to EIA 11 has been built under the proposed National Economic Development alignment and the restoration of Ponds A9 through A18 are identical to those assumed in the Year 50 conditions for the EIA 11 study (MacWilliams et al. 2012). As a result, the Year 50 bathymetry and restoration geometry developed for the SSFBSS for EIA 11 was applied to all Year 50 existing conditions scenarios for this study.

5.3 Water Surface Evaluation Locations for Existing Conditions Scenarios

Predicted water surface elevations for each of the 180 Year 0 existing conditions scenarios and the 540 Year 50 existing conditions scenarios were evaluated at 69 stations spanning from EIA 1 through EIA 10 (Figure 5.3-1). Thirty-eight of the evaluation locations are located seaward of the proposed project levee alignment. The remaining 31 evaluation locations are located behind the proposed project levee alignment to evaluate flood risk in each EIA behind the proposed project levee. Fourteen evaluation stations are located immediately adjacent to the proposed project levee alignment. For each scenario, lookup tables were developed to provide the maximum water surface elevation at each of the 69 locations for each of the 720 existing conditions scenarios simulated, resulting in a total of 49,680 predictions of maximum water surface elevations under existing conditions. These predictions of maximum water surface elevation were used by Noble Consultants in the Monte Carlo simulations in order to develop the flood frequency curves at each of the 69 locations as part of this study. The results of the Monte Carlo simulations and the resulting flood frequency curves at each location are presented in a separate report prepared by Noble Consultants.

Figure 5.3-1
Locations used for evaluation of peak water surface elevations for the existing conditions scenarios (Black lines are creek and pond levees and the green line is the extent of the model grid.)

6 SIMULATION OF WITH-PROJECT CONDITIONS FOR YEAR 0 AND YEAR 50

This section provides a description of the modeling assumptions and boundary conditions for the with-project scenarios. A total of 360 scenarios were developed to span the range of hydrodynamic parameters for with-project conditions for Year 0 and Year 50.

6.1 Scenario Matrix and Modeling Assumptions for Year 0 With-Project Simulations

The primary difference between the Year 0 with-project conditions scenarios and the Year 0 existing conditions scenarios is the construction of the project levee (Figure 6.1-1). In all with-project scenarios, it is assumed that the project levee does not overtop or fail (breach). In addition, it is assumed that there are no failures or overtopping of the creek levees within the project area, because the focus of this study is restricted to coastal flooding.

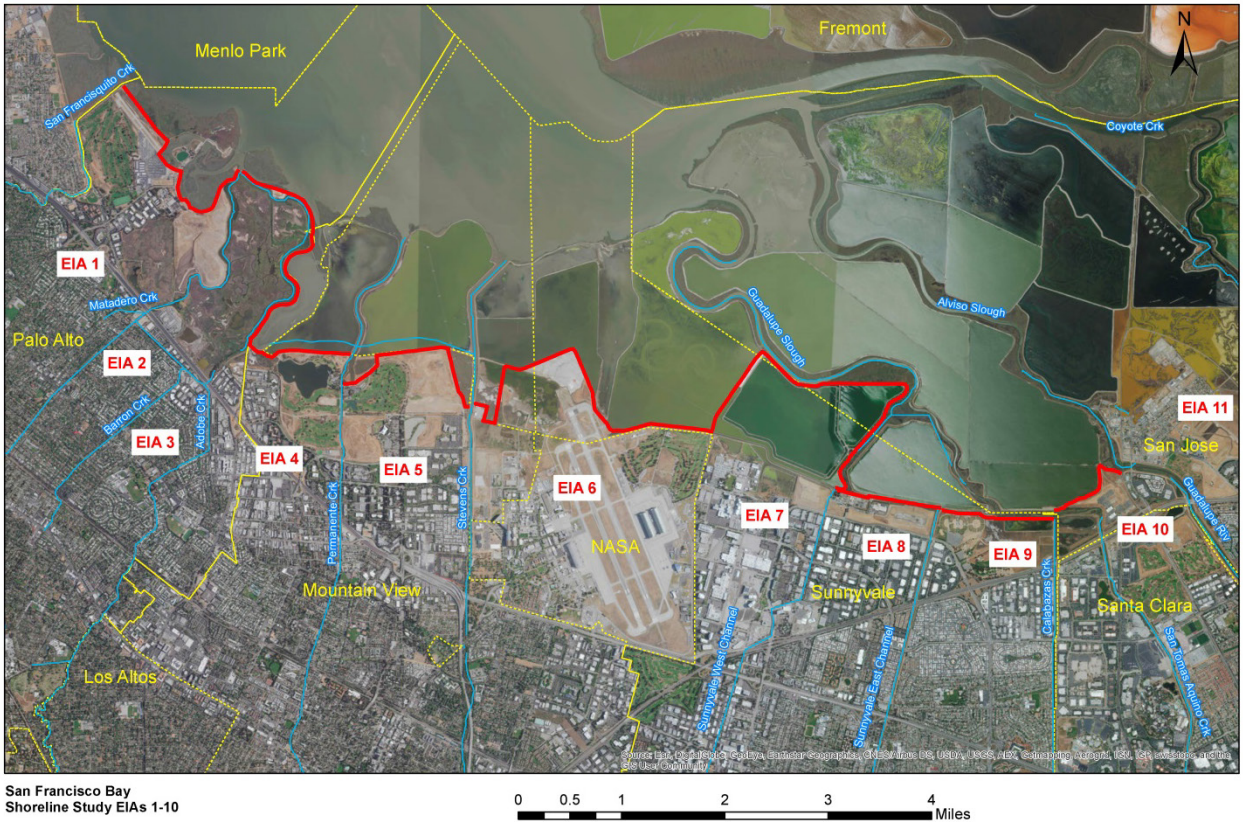

Figure 6.1-1

Alignment of project levee (red) for EIAs 1 through 10

6.1.1 Description of Year 0 With-Project Scenarios

A total of 144 scenarios were conducted for Year 0 with-project conditions. The Year 0 with-project conditions scenarios were developed using the 12 water level and flow events, 6 wind combinations, and 5 breach zones (Table 6-1). The first set of 36 scenarios consists of 12 scenarios representing the combined tide and surge for Events 1 through 12 (Table 4-1) with no wind. The remaining 24 of the 36 scenarios were designed to determine the contribution of wind to the peak water surface elevation for a range of wind speeds and directions. These 24 scenarios use the tidal forcing for four events (1, 3, 10, and 12) with 6 different combinations of wind speed and direction (Table 4-4). The combination of no-wind and with-wind scenarios results in a total of 36 scenarios for Year 0 with-project, with no inner or outer levee breaches.

Table 6-1
Year 0 With-Project Scenarios

With-Project Scenario	Year	SLR Rate	Inner Breaches	Outer Breaches	Number of Scenarios
With-Project Levee Alignment	0	None	None	None	36
				EIA 1 to EIA 3	0
				EIA 4 & EIA 5	36
				EIA 6 & EIA 7	36
				EIA 8 & EIA 9	36
				EIA 10	0
Total Number of Year 0 With-Project Scenarios					**144**

Notes:
EIA = Economic Interest Area
SLR = sea level rise

In the Year 0 with-project conditions, it was assumed that there were no inner levee failures along the project levee; however, breach scenarios were considered with included breaches in the outer levees (Table 6-1). Due to the project levee alignment in front of EIA 1 to EIA 3, there were no locations at which outer levee failures could occur under with-project conditions in Breach Zone 1; however, outer levee breaches were considered for EIAs 4 through 9 (Figure 6.1-1), resulting in a total of 108 outer breach scenarios (Table 6-1).

Figure 6.1-2
Levee breach locations for each breach zone for Year 0 with-project conditions (Black lines are creek and pond levees and the magenta line is the proposed project levee alignment.)

6.1.2 Salt Pond Operations and Water Surface Elevations for Year 0 With-Project Scenarios

Because the assumed base year for Year 0 conditions for this project is 2017, the Year 0 scenarios assume that the salt ponds are operated similarly to how they are currently operated during winter, and that further restoration of these ponds has not yet begun in Year 0. The operations of the Salt Ponds bayward of EIA 1 through EIA 11 for Year 0 with-project conditions are assumed to be identical to the pond operations for Year 0 conditions described for existing conditions in Section 5.1.2.

6.2 Scenario Matrix and Modeling Assumptions for Year 50 With-Project Simulations

6.2.1 Description of Year 50 With-Project Scenarios

A total of 216 scenarios were conducted to determine the peak water levels for Year 50 with-project conditions. The horizontal grid for the Year 50 with-project conditions was identical to the Year 0 with-project scenarios, with the assumed project levee alignment and

the adjacent creek levees assumed to be high enough under with-project conditions that they do not over top or fail in any scenarios. The creek inflows and wind were also identical to the Year 0 with-project scenarios.

For Year 50 conditions, SLR was calculated between 2017 and 2067 using the USACE Low Curve, the USACE Intermediate Curve, and the USACE High Curve, as described in Section 4.4. Based on these projections, the Year 50 scenarios were designed by adjusting relative sea level upward by 0.51 ft between 1992 and 2067 for the USACE Low Curve, 1.01 ft between 1992 and 2067 for the USACE Intermediate Curve, and 2.59 ft between 1992 and 2067 for the USACE High Curve. The Year 50 with-project scenarios include a set of 36 no-breach scenarios for each of the three different SLR curves described in Section 4.4 (Table 6-2). In the Year 50 with-project conditions, it was assumed that there were no inner levee failures along the project levee; however, breach scenarios were considered that included breaches in the outer levees of the ponds that remain as managed ponds in Year 50 (Table 6-2). In the Year 50 with-project conditions, outer levee breaches were considered for EIA 6 and EIA 8 (Figure 6.2-1), resulting in a total of 36 outer breach scenarios for each SLR rate (Table 6-2).

Table 6-2
Year 50 With-Project Scenarios

With-Project Scenario	Year	SLR Rate	Inner Breaches	Outer Breaches	Number of Scenarios
With-Project Levee Alignment	50	USACE Low Curve	None	None	36
				EIA 6 & EIA 8	36
With-Project Levee Alignment	50	USACE Intermediate Curve	None	None	36
				EIA 6 & EIA 8	36
With-Project Levee Alignment	50	USACE High Curve	None	None	36
				EIA 6 & EIA 8	36
Total Number of Year 50 With-Project Scenarios					**216**

Notes:
SLR = sea level rise
USACE = U.S. Army Corps of Engineers

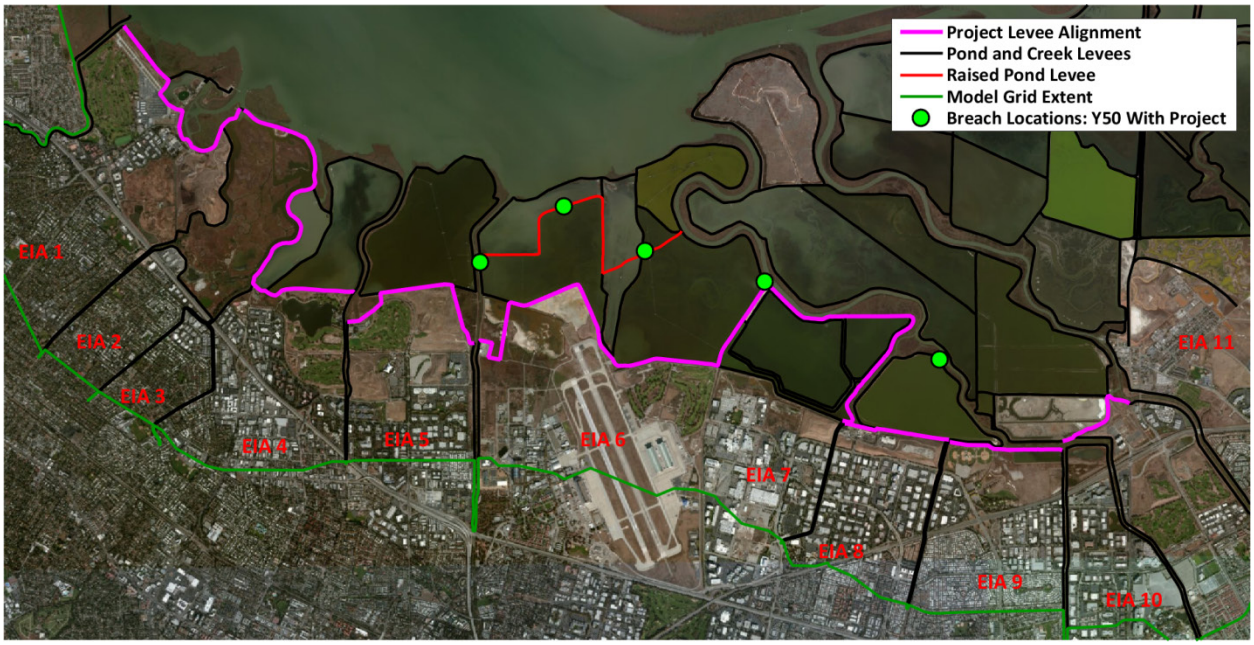

Figure 6.2-1
Levee breach locations for each breach zone for Year 50 with-project conditions. Black lines are creek and pond levees and the magenta line is the proposed project levee alignment.

6.2.2 Salt Pond Operations and Water Surface Elevations for Year 50 With-Project Scenarios

The Year 50 with-project scenarios assume that phased restoration of the South Bay salt ponds occurs between Year 0 (2017) and Year 50 (2067). The phased restoration assumes that Ponds A1 and A2W are restored in 2020, Ponds A5, A7, A8, and A8S are restored in 2025, Pond A3N is restored in 2030, and Ponds A2E, AB1, and portions of Ponds AB2 and A3W are restored in 2040 (Table 6-3). It is assumed that Ponds A2E, portions of Ponds AB2 and A3W, and Pond A4 remain as managed ponds in Year 50 (Figure 6.2-2).

Table 6-3
South Bay Salt Pond Restoration Phasing Assumed for Year 50 With-Project Scenarios

Pond	Breach Year
A1	2020
A2W	2020
A5	2025
A7	2025

A8	2025
A8S	2025
A3N	2030
A2E	2040
AB1	2040
AB2 (Partial)	2040
A3W (Partial)	2040

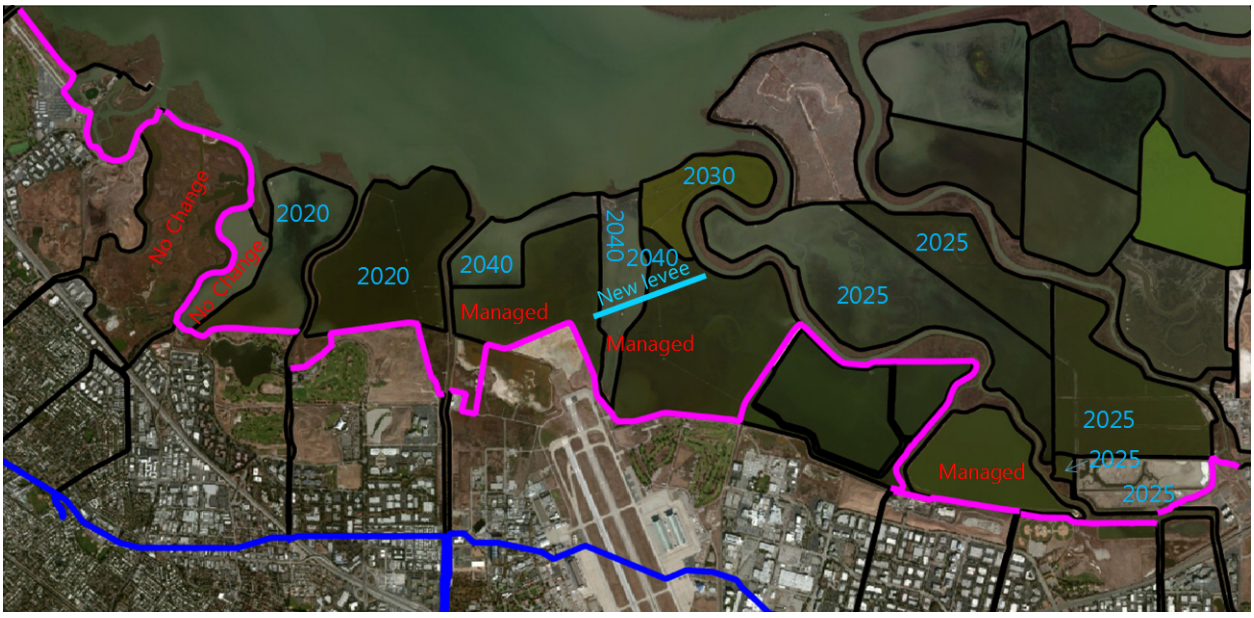

Figure 6.2-2
South Bay salt pond restoration phasing assumed for Year 50 with-project scenarios

6.2.2.1 Palo Alto Flood Basin and Inner Charleston Slough

The Year 50 with-project conditions assumed that no changes were made to the operation of the PAFB or ICS. Operations for both the PAFB and ICS for Year 50 with-project conditions (see Figure 6.2-5) were assumed to be identical to those described for Year 0 existing conditions in Section 5.1.2.1.

6.2.2.2 Restoration Assumptions for Ponds A1 and A2W

The Year 50 conditions assume that restoration of Ponds A1 and A2W occurred in 2020. Marsh accretion within Pond A1 and Pond A2W between 2020 and 2067 was calculated as described in Section 6.2.3. Restoration of Pond A1 included a breach on the east and west

side of Pond A1 with channels extending from each breach into the pond in Year 50, and some portions of the levee lowered (Figure 6.2-3). Restoration of Pond A2W included two breaches on both the east and west side of Pond A2W with channels extending form each breach into the pond in Year 50, and some portions of the western levee lowered (Figure 6.2-3).

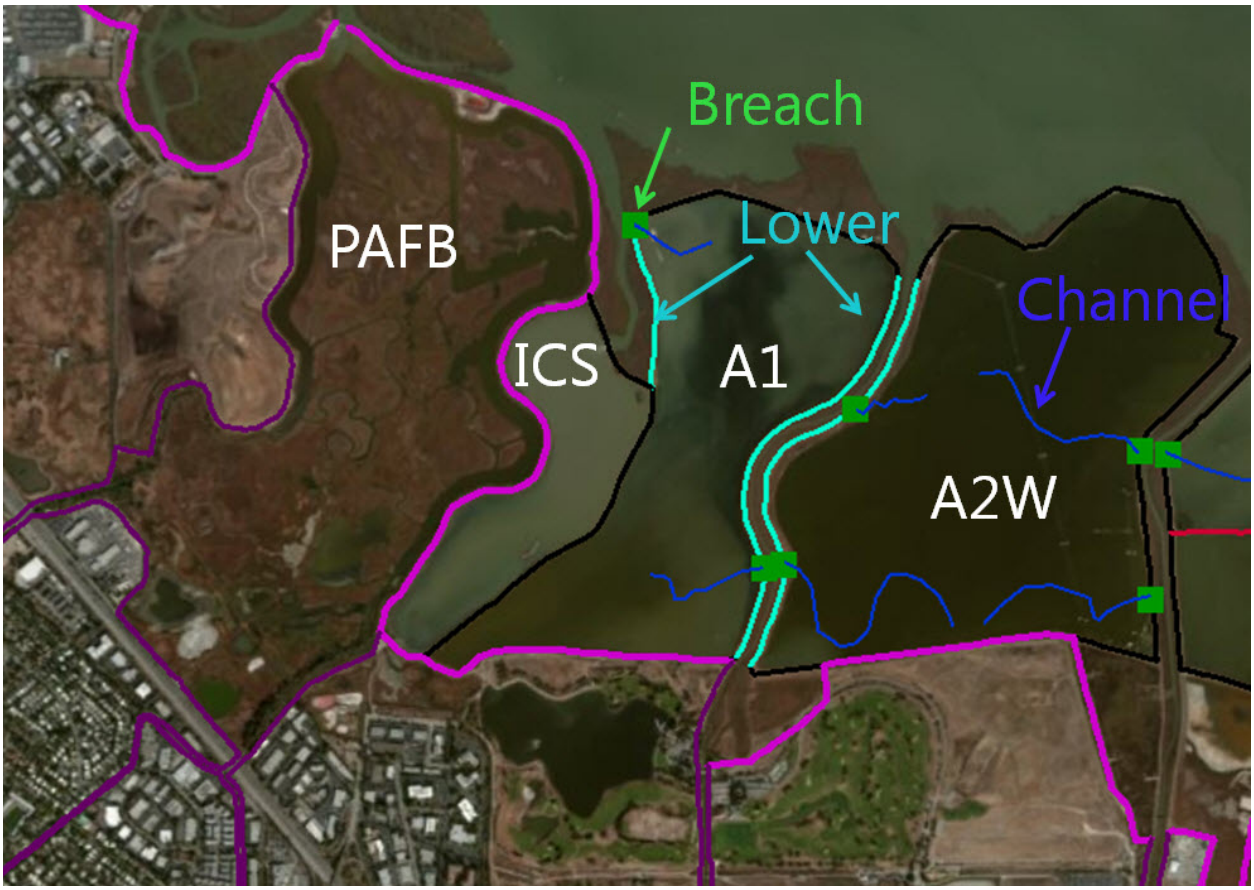

Figure 6.2-3
Restoration assumptions for Ponds A1 and A2W

6.2.2.3 Restoration Assumptions for Ponds AB1 to A3W

The Year 50 conditions assume that restoration of Pond A3N occurred in 2030 and restoration of Pond AB1 and portions of Pond AB2 and A3W occurred in 2040. Marsh accretion within Pond A3N, Pond AB1, and the restored portions of Pond AB2 and Pond A3W between the year of restoration and 2067 was calculated as described in Section 6.2.3. Restoration of Pond A3N included two breaches in the east side of the pond along Guadalupe

Slough and lowering of a portion of levee adjacent to the breaches (Figure 6.2-4). As part of the subsequent restoration of portions of Pond AB2 and Pond A3W, the levees between the restored portions of Ponds A3N, AB2, and A3W were also lowered and a breach was constructed on the northern side of Pond AB2. Restoration of Pond AB1 included a breach on the west side and lowering of the levee between Pond AB1 and AB2 (Figure 6.2-4). Because Pond A2E and portions of Pond AB2 and A3W were assumed to remain managed ponds in Year 50, the levee between Pond A2E and Pond AB1 and a portion of Pond AB2 was raised and a new levee was constructed across Ponds AB2 and A3W (Figure 6.2-4). The crest elevation of the constructed levee was assumed to be 13 feet NAVD88 such that the raised and new levees provide an equivalent level of protection to the existing levee north of Ponds AB1 and AB2.

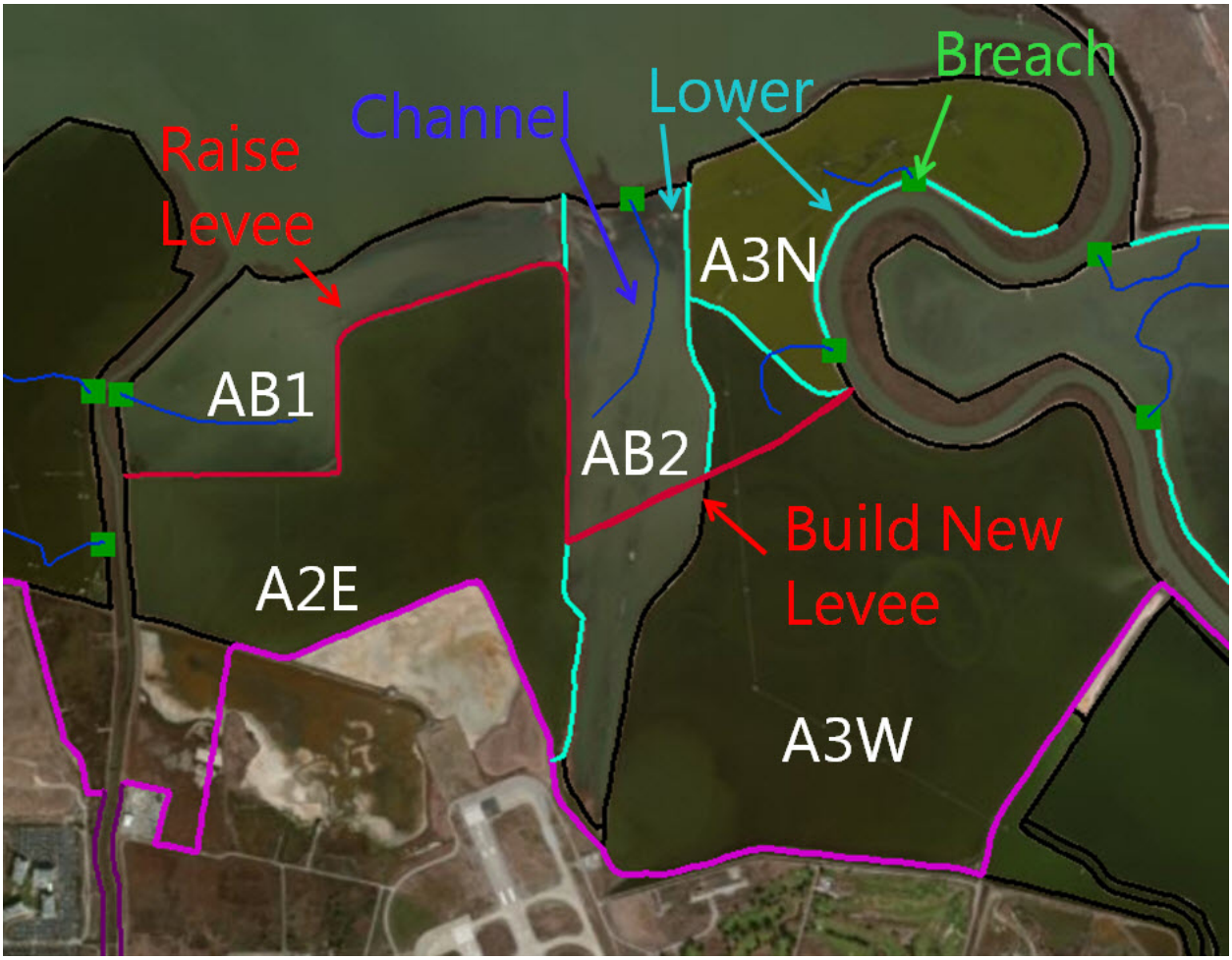

Figure 6.2-4

Restoration assumptions for Ponds AB1, AB2, A3W, and A3N

6.2.2.4 Managed Pond Operation Assumptions for Ponds A2E, A3W, and A4

Under Year 50 with-project conditions, Pond A2E was expanded to include the southern portion of Pond AB2. A new inlet structure was constructed between Stevens Creek and Pond A2E, and the existing structure between Pond AB1 and A2E was assumed to be closed. The new structure between Stevens Creek and Pond A2E was assumed to consist of one bidirectional 48-inch pipe, and one 48-inch pipe with a flap gate that allows for only unidirectional flow into Pond A2E (Figure 6.2-5). The existing 36-inch gate between the southern part of Pond AB2 and Pond A3W is assumed to be enlarged to a 48-inch gate. The outlet from Pond A3W to Guadalupe Slough is assumed to remain unchanged, with three 48-inch pipes allowing unidirectional flow out of Pond A3W to Guadalupe Slough. Under existing conditions, there is a 72-inch siphon between Pond A4 and the east end of the Cargill channel, and there is an opening that allows flow between Pond A3W and the western end of this channel. Through these connections, water levels in Pond A4 are effectively controlled by water levels in Pond A3W. Because the Cargill channel is behind the project levee, the Year 50 scenarios assume a direct siphon between Pond A4 and Pond A3W to eliminate any possibility of flooding behind the project levee. This allows Pond A4 to continue to operate as it does under current conditions; however, a direct siphon between Pond A4 and Pond A3W is not likely to be cost-effective. This assumption was necessary, because in any scenarios when the outer levees of Pond A4 overtopped, flow from the siphon into the Cargill channel could allow for flooding behind the project levee. To address this issue, it may be necessary to raise the levee along the south side of the Cargill channel that currently connects Pond A4 to A3W, or to establish a different management regime for Pond A4 that includes a direct connection to Guadalupe Slough.

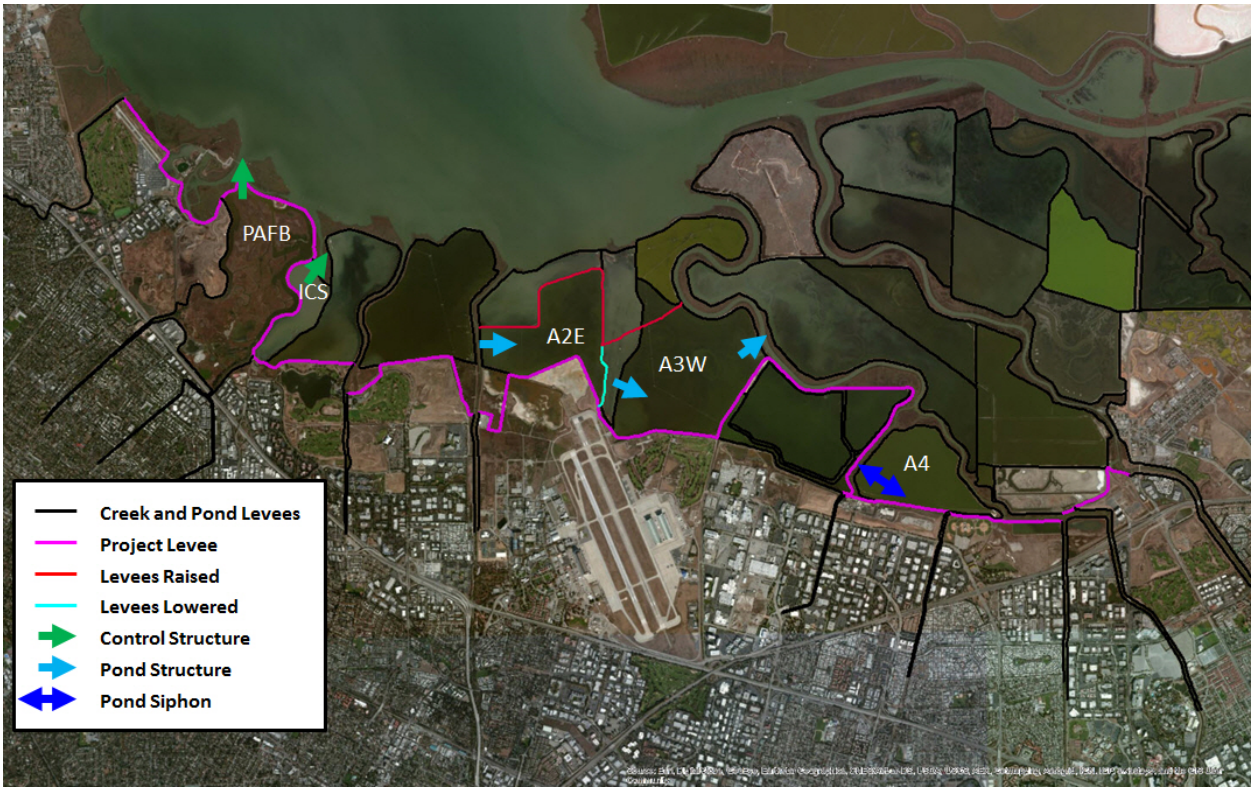

Figure 6.2-5
Locations of control structures and siphons for the Palo Alto Flood Basin (PAFB), Inner Charleston Slough (ICS), and Ponds A2E, A3W, and A4, which remain as managed ponds under Year 50 with-project conditions

6.2.2.5 Restoration Assumptions for Ponds A5, A7, A8, and A8S

The Year 50 conditions assume that restoration of Ponds A5, A7, A8, and A8S occurred in 2025. Marsh accretion within Ponds A5, A7, A8, and A8S between 2025 and 2067 was calculated as described in Section 6.2.3. Restoration of Pond A5 included four breaches along Guadalupe Slough, with channels extending from each breach into the pond. Two portions of the western levee of Pond A5 along Guadalupe Slough were assumed to be lowered to marsh plain elevation (Figure 6.2-6). Restoration of Pond A7 included two breaches along Alviso Slough, with channels extending from each breach into the pond. Two portions of the eastern levee of Pond A7 along Alviso Slough were assumed to be lowered to marsh plain elevation (Figure 6.2-6). Restoration of Pond A8 included one breach along Alviso Slough, with a channel extending from the breach into the pond (Figure 6.2-6). Restoration of Pond A8S included one breach in the southern levee near the junction of San Tomas Aquino Creek

and Calabasas Creek, with a channel extending from the breach into the pond. The restoration of this pond group included multiple internal levee breaches, and also assumed lowering of the levee south of Pond A6 to 2 ft above marsh plain, with one opening at marsh plain elevation connecting Pond A6 to both Pond A5 and A7 (Figure 6.2-6).

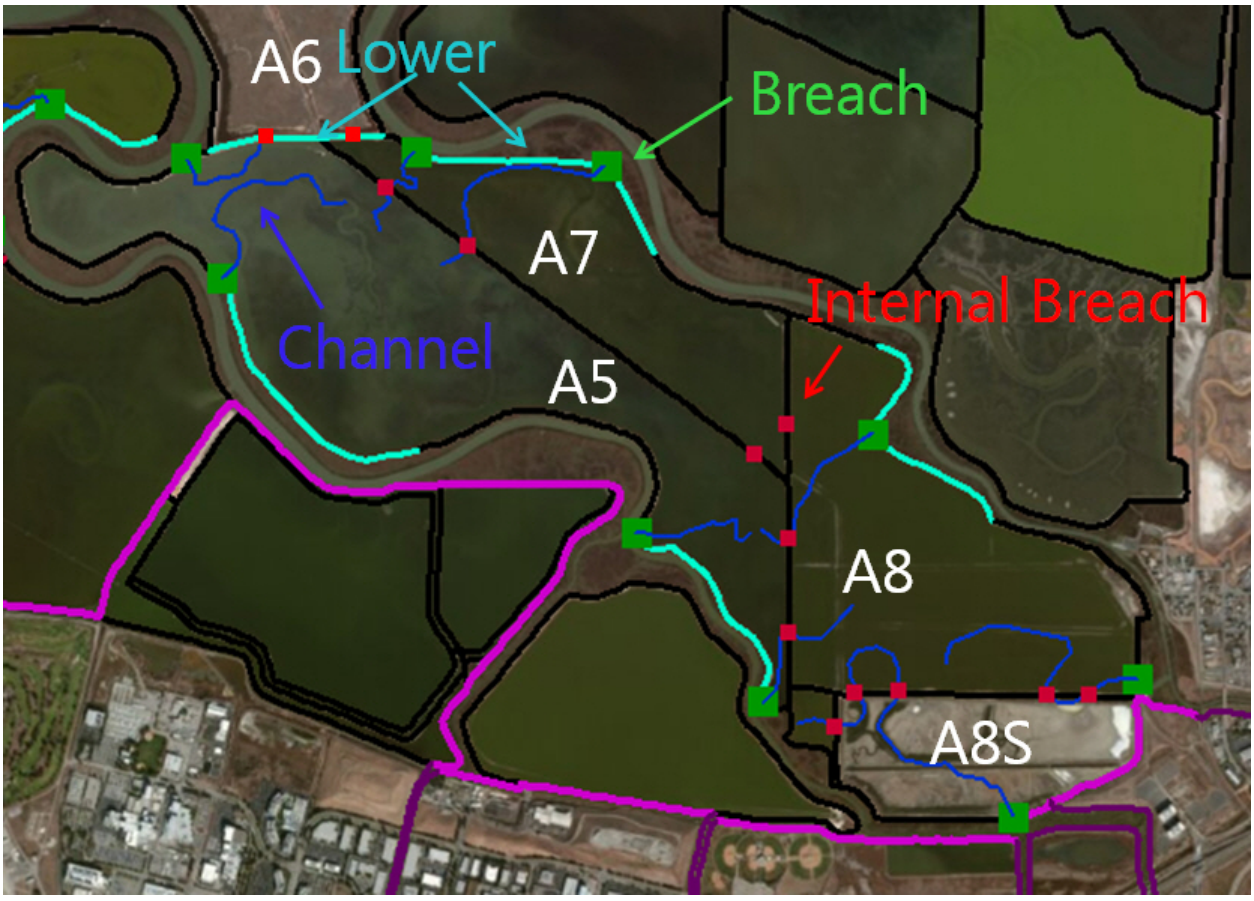

Figure 6.2-6
Restoration assumptions for Ponds A5, A7, A8, and A8S

6.2.2.6 Restoration Assumptions for Ponds A9 to A18

The Year 50 restoration assumptions for Ponds A9 through A15 are identical to those used for the SSFBSS Study (MacWilliams et al. 2012). The Year 50 bathymetry and restoration geometry developed for the SSFBSS Study, which was applied to the Year 50 existing conditions scenarios as described in Section 5.2.2, also was applied to all Year 50 with-project scenarios for this study.

6.2.3 Marsh Accretion Modeling for Year 50 With-Project Conditions

Numerical models can be applied to predict elevation changes within salt marshes and restored ponds for scenarios including SLR, changes in sediment input, and other environmental forcings (French 1993; Allen 1995; Callaway et al. 1996; Morris et al. 2002; Williams and Orr 2002; French 2006; Kirwan and Murray 2007; D'Alpaos 2011). In this study, the Wetland Accretion Rate Model for Ecosystem Resilience (WARMER) model was applied to estimate the accretion that would occur within each restored salt pond between the year that each pond was restored and 2067, which is the assumed year for the Year 50 scenarios.

6.2.3.1 Description of WARMER model

WARMER is a 1-D model of marsh elevation that incorporates both biological and physical processes resulting in vertical marsh accretion. The WARMER model has been applied to evaluate the habitat evolution of marshes in the San Francisco Estuary and the Sacramento-San Joaquin Delta (Swanson et al. 2014; Swanson et al. 2015). WARMER is a computationally efficient 1-D model that captures the dynamics of critical marsh accretion processes in wetlands with input functions defined either estuary-wide or based on individual sites. WARMER is a 1-D Cohort model of wetland accretion based on the Callaway et al. (1996) model, hereafter the Callaway model (Figure 6.2-7). The Callaway model calculates changes in elevation relative to mean sea level (MSL) of a unit area representative of the marsh surface. These changes in marsh elevation are based on changes in relative sea level, subsidence, a linear inorganic sediment accumulation function, constant aboveground and below ground organic matter productivity, and compaction and decay. WARMER improves upon the Callaway model by including inundation-based sediment and organic matter accumulation functions and a temporally-variable rate of SLR.

The elevation computed in WARMER of the marsh surface E, at time t relative to local MSL is as follows:

$$E(t) = E(0) - SLR(t) + \sum_{i=0}^{t} V_i\,(t) \qquad (1)$$

where E(0) is the initial elevation relative to MSL, SLR(t) is the sea level at time t relative to the initial sea level and $V_i(t)$ is the volume per unit area, or height, at time t, of the cohort formed during Year i. The total volume of an individual cohort is the sum of the mass of water, which is calculated from the porosity of the cohort, the mass of sediment, and the mass of organic matter divided by the cohort bulk density.

Each modeled annual cohort contains the mass of inorganic and organic matter accumulated at the surface in a single year with any subsequent belowground organic matter productivity (root growth), less decay. Cohort density, a function of mineral, organic, and water content, is calculated at each time step to account for decay of organic material and autocompaction of the soil column. The change in relative elevation is then equal to the difference between the change in modeled sea level and the change in height of the soil column, which is the sum of the volume of all cohorts over the unit area model domain.

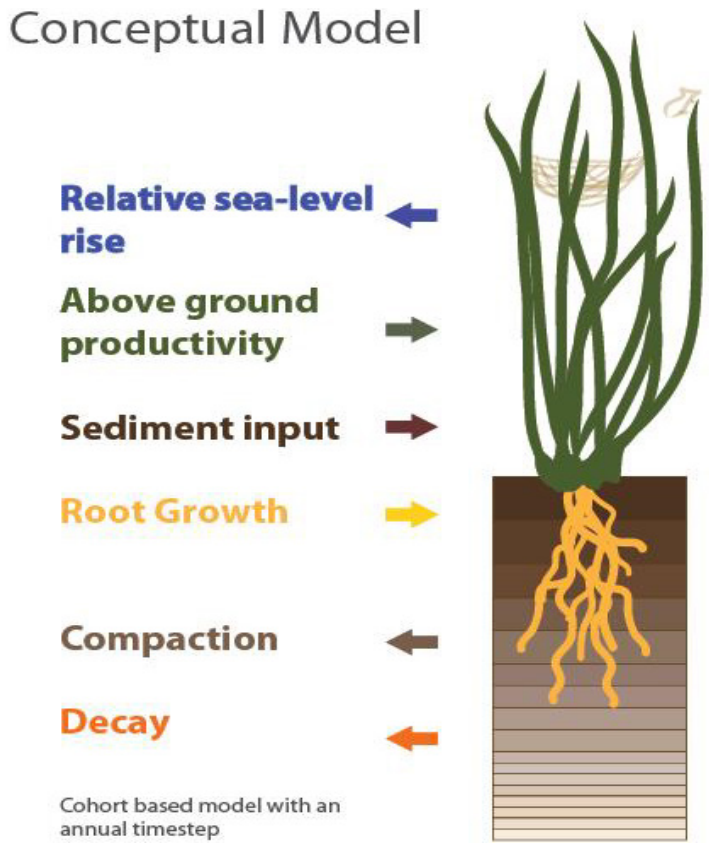

Figure 6.2-7
Conceptual model for WARMER marsh accretion model and inputs (The direction of the arrow between inputs and the figure indicates whether the process increases or decreases the relative elevation of the marsh surface.)

Because WARMER is a 1-D model in the vertical direction, it is applied to a number of initial elevations representative of the topography or bathymetry of the project area. The final marsh elevation for points with initial elevations between modeled elevation points are linearly interpolated between the modeled points to create a full DEM of the final elevation of the project area for each scenario.

6.2.3.2 WARMER Model Inputs

WARMER has been previously calibrated to evaluate San Francisco Bay tidal marsh response to SLR (Swanson et al. 2014). The model was validated by applying the historic rate of SLR for the calibrated model and comparing the modeled and observed soil column profiles (bulk density and organic matter content). The calibrated marsh accretion parameters for sediment

and organic matter accumulation from Whale's Tail Marsh and physical characteristics from Laumeister Marsh in South San Francisco Bay from Swanson et al. (2014) were applied in this study to evaluate the landscape evolution for breached salt ponds in that same region of the Bay. A full listing of model parameters can be found in Swanson et al. (2014). The calibrated sediment accumulation function used in WARMER for South San Francisco Bay is shown in Figure 6.2-8. Sediment flux from the water column to the marsh surface at a given elevation is equal to the product of suspended solids concentration (SSC), and settling velocity summed over all times that elevation z is inundated. For the case of constant SSC and settling velocity, the mass accumulation is directly proportional to the inundation frequency. No accumulation takes place above the observed maximum annual tide (MAT) and all elevations below the minimum observed tide level receive the same amount of sediment.

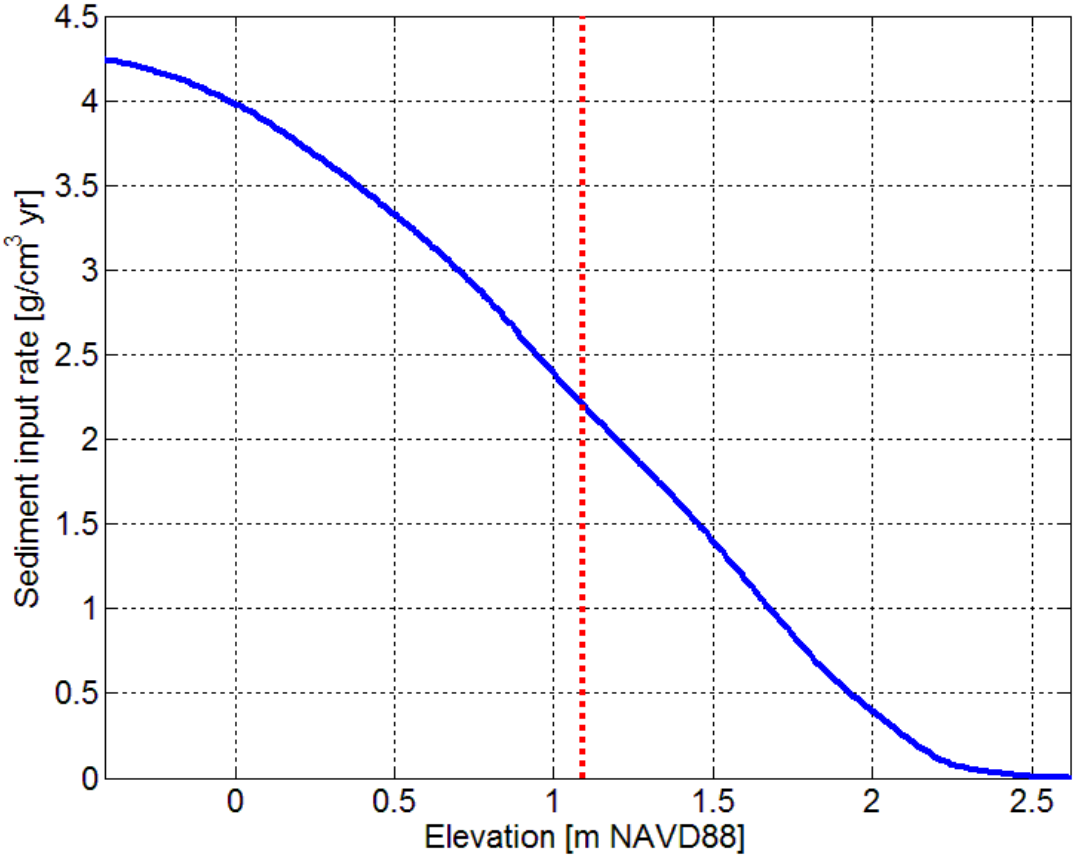

Figure 6.2-8
Sediment accumulation function for South San Francisco Bay (blue) at the beginning of the simulation period relative to NAVD88. MSL is shown as a dotted red line.

Because the tidal marshes in the San Francisco Estuary selected for this study are dominated by *Sarcocornia pacifica*, the organic input function developed by Morris et al (2002) for *Spartina alterniflora* was adapted to this dominant plant species. The shape of the parabolic curve that Morris et al. (2002) developed for *S. alterniflora* salt marshes was confirmed for other salt marsh species (Kirwan and Guntersbergen 2012) and was retained for this study, but the elevation range of vegetation, the roots of the parabolic equation, and the magnitude of organic matter input are adjusted for San Francisco Estuary marsh vegetation, primarily *S. pacifica*, as described in Swanson et al. (2014). The total organic matter accumulation function is shown in Figure 6.2-9. No organic matter accumulation occurs when the surface elevation is above MAT or below MSL.

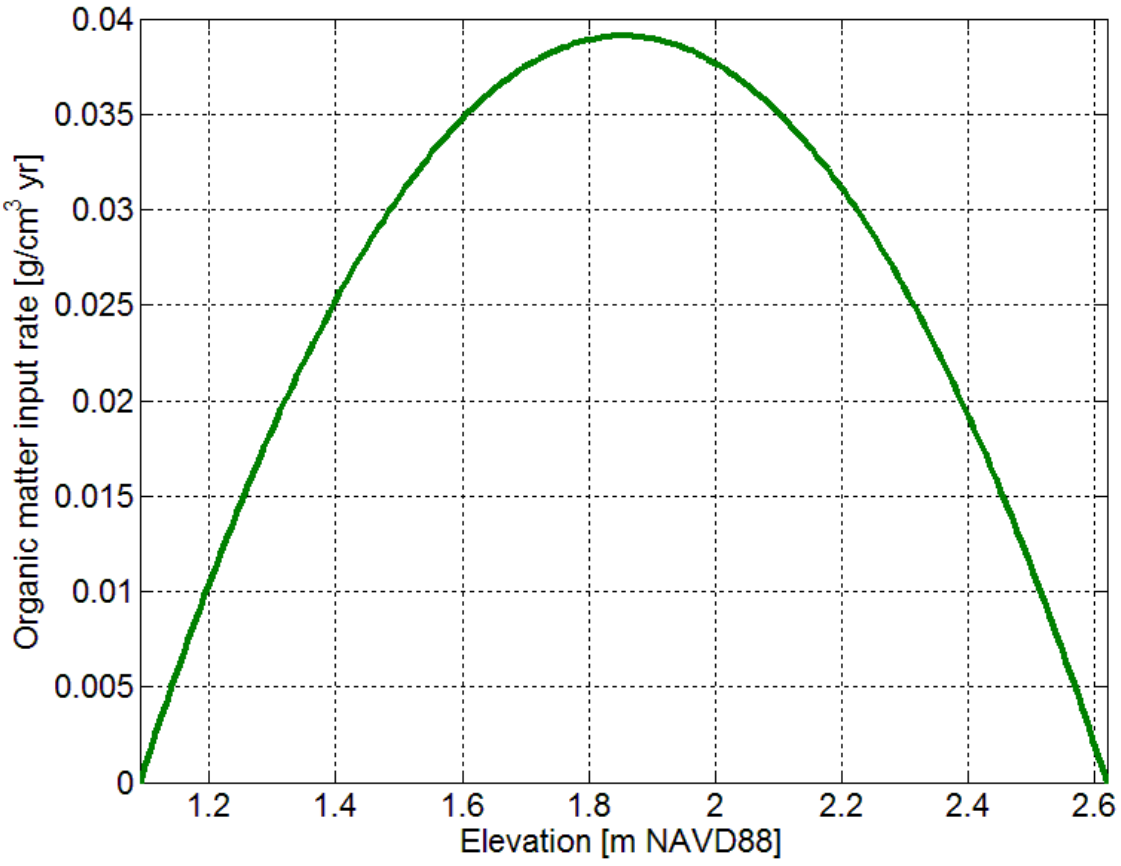

Figure 6.2-9
Total organic matter accumulation as a function of elevation (NAVD88) at the beginning of the simulation period

6.2.3.3 WARMER Scenarios

Because the rate of accretion depends on the rate of SLR, separate WARMER scenarios were simulated for the USACE Low Curve, the USACE Intermediate Curve, and the USACE High Curve, as described in Section 4.4. The WARMER scenarios were designed assuming 0.51 ft, 1.01 ft, and 2.59 ft of SLR between 1992 and 2067 for the USACE Low, Intermediate, and High SLR curves, respectively (Figure 6.2-10).

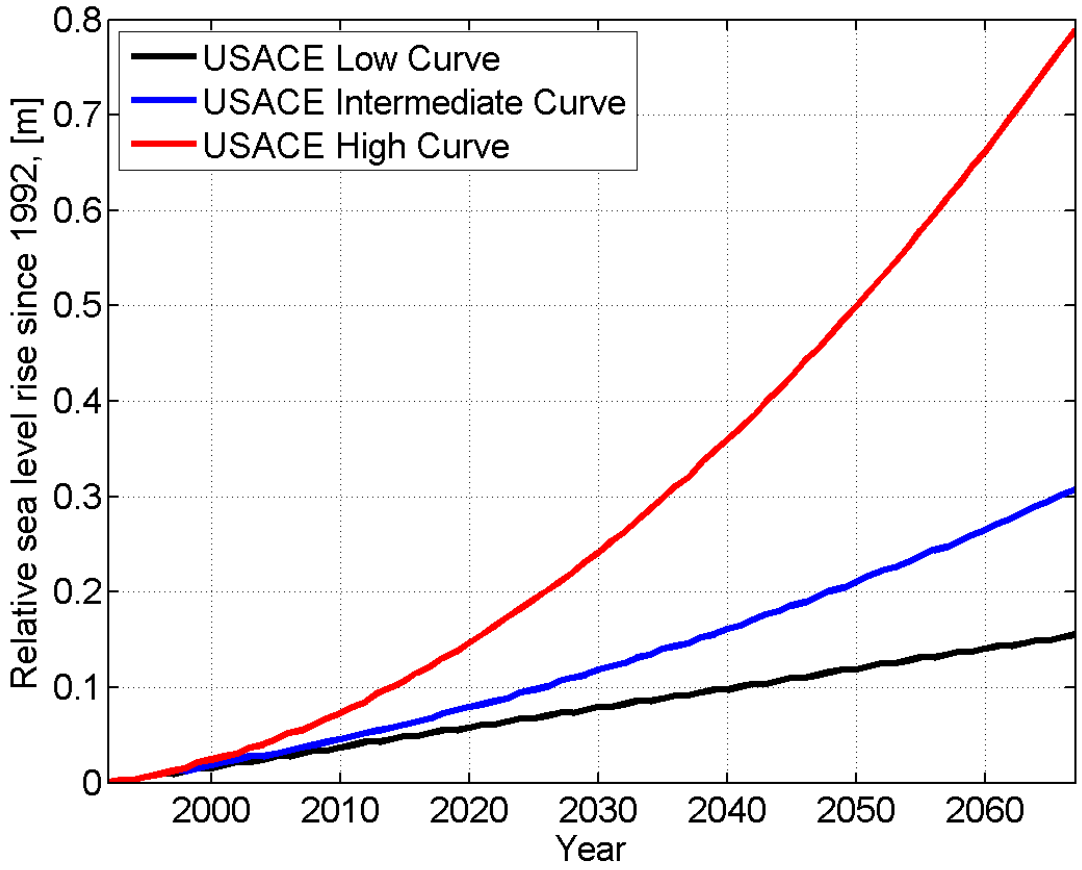

Figure 6.2-10
Project sea level projections relative to MSL in 1992 for USACE Low Curve, USACE Intermediate Curve, and USACE High Curve

For Ponds A6, A17, A19, A20, and A21, accretion was calculated between 2010 (the year the bathymetry data for those ponds was collected) and 2067. For the remaining ponds, which were assumed to be restored between Year 0 and Year 50, accretion was calculated between the breach year (Table 6-3 and Figure 6.2-2) and 2067. For ponds that remained managed

ponds in 2067 (Pond A4, A2E, and portions of Ponds AB2 and A3W), no accretion was assumed between 2017 and 2067. No accretion was also assumed in the PAFB and ICS because there is assumed to be no change in operation of those basins in the Year 50 scenarios.

Initial elevations relative to MSL for existing marshes and ponds within the project area that are currently breached or assumed to be breached between 2017 and 2067 were determined from bathymetry of the ponds described in Section 3.4. The bathymetry data were acquired in 2010 and 2011 and are referenced in NAVD88.

Seven elevations ranging from -2.0 to 4.0 m NAVD88 at 1.0 m increments were chosen as representative marsh and pond elevations and were modeled for each SLR curve and breach year. These elevations span the range of initial and final elevations within the ponds that would potentially accumulate sediment from tidal inundation during the simulation period. The accretion at each of these elevations at the end of the simulation period was determined from the change in soil column depth. Total accretion at all elevations within each pond between adjacent modeled elevations was determined by linear interpolation. The few points with elevations above 4.0 m NAVD88 or below -2.0 m NAVD88 were assumed to accumulate the same amount of soil as the 4.0 m NAVD88 or -2.0 m NAVD88 elevations, respectively.

6.2.3.4 WARMER Results

WARMER was applied for a total of 126 scenarios as defined by initial elevation, breach year, and SLR curve. Total accretion of sediment and organic matter for each SLR curve and breach year is plotted in Figures 6.2-11 through 6.2-13. Accretion was largest for the lowest initial elevations and the most rapid SLR due to the inverse relationship between sediment accumulation and elevation. Ponds with earlier breach years also had greater accretion due to the increased time of tidal inundation during the simulation period. Figure 6.2-14 shows initial elevations within the study area in each of the ponds for which accretion was calculated. Figures 6.2-15, 6.2-16, and 6.2-17 show the 2067 elevations predicted using WARMER for the USACE Low, USACE Intermediate, and USACE High SLR curves, respectively.

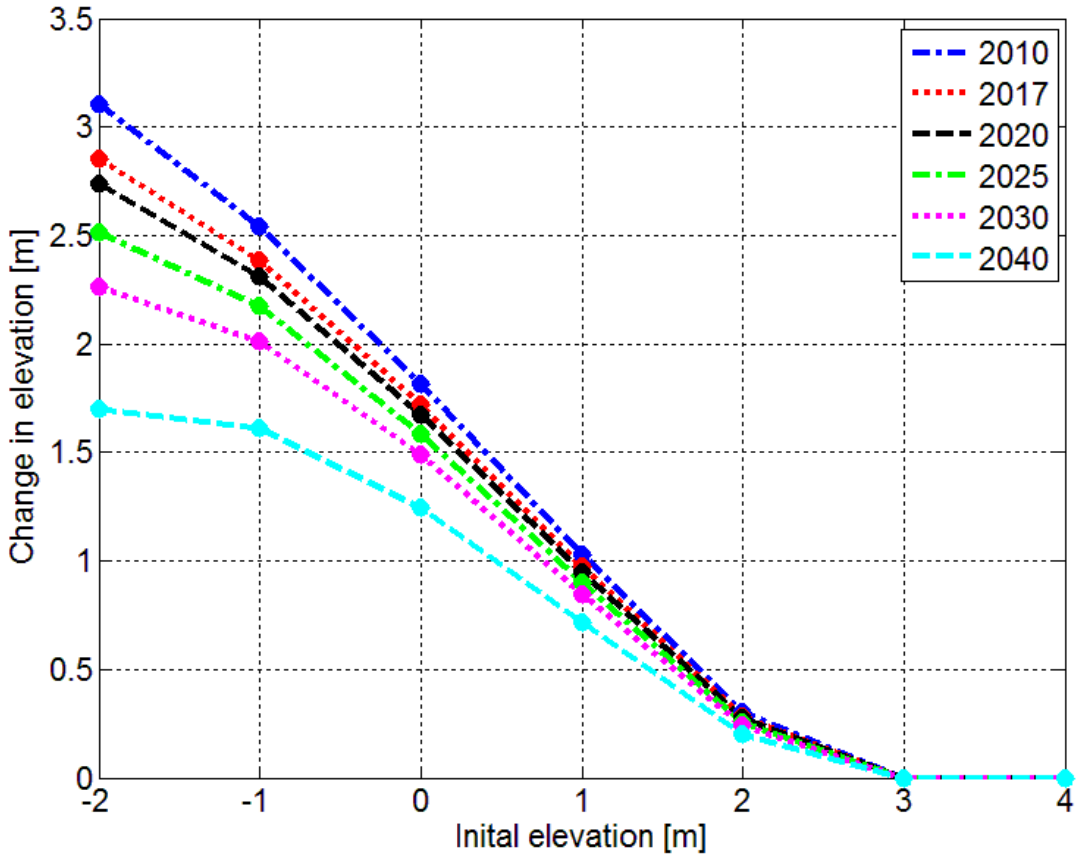

Figure 6.2-11

Accretion as a function of initial elevation and breach year for USACE Low Curve

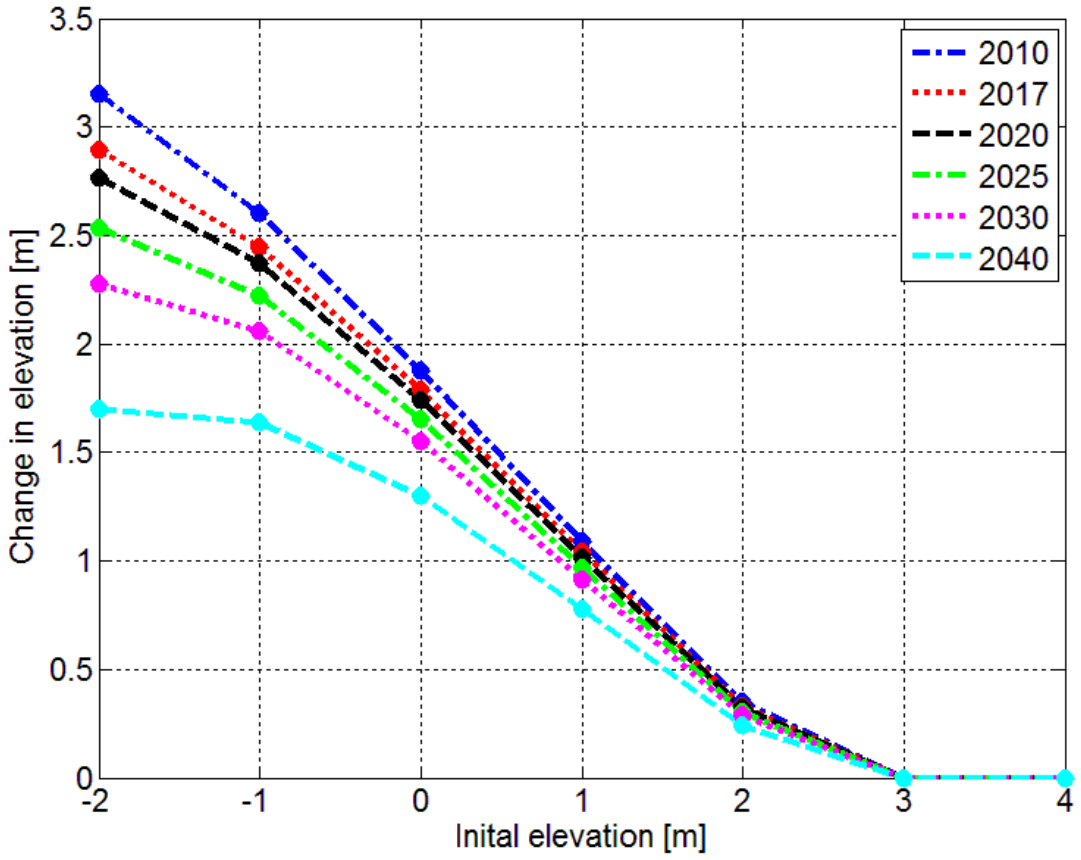

Figure 6.2-12

Accretion as a function of initial elevation and breach year for USACE Intermediate Curve

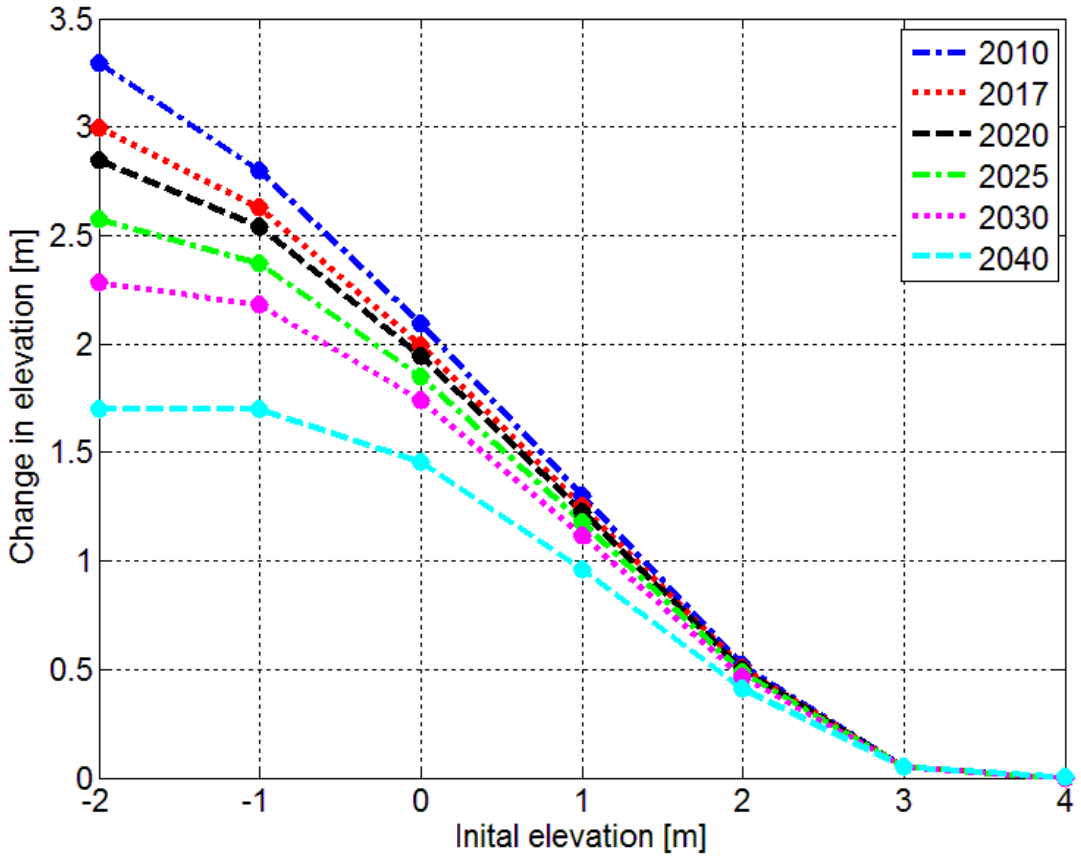

Figure 6.2-13

Accretion as a function of initial elevation and breach year for USACE High Curve

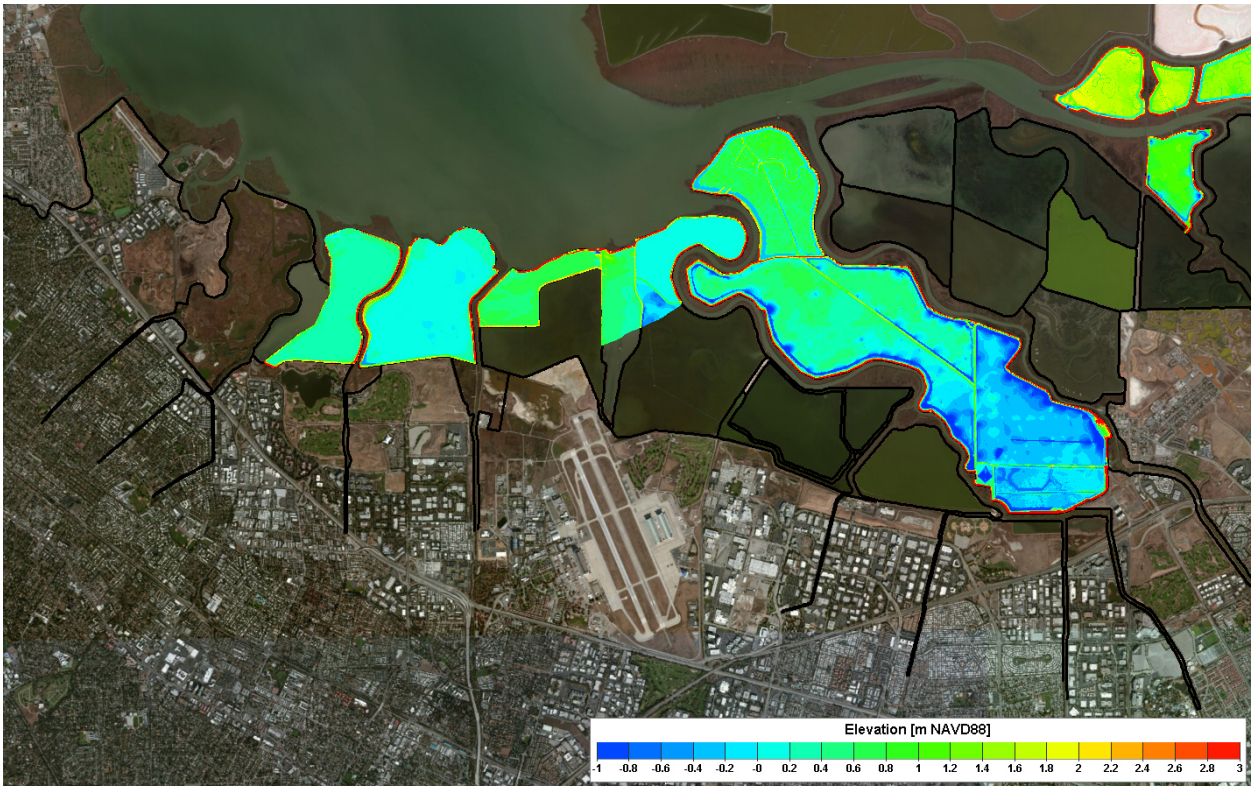

Figure 6.2-14

Initial elevations in meters NAVD88 within restored ponds in which accretion for year 2067 was calculated using the WARMER model

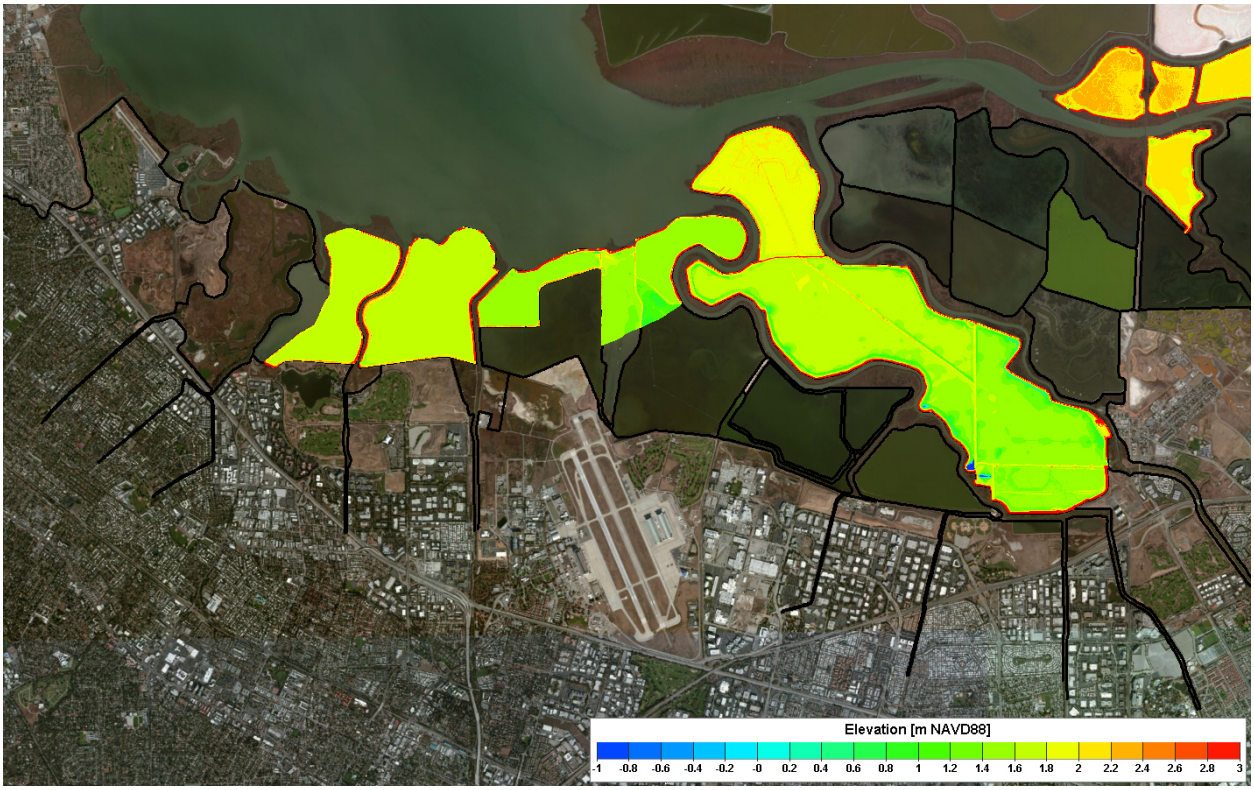

Figure 6.2-15

Final 2067 elevations in meters NAVD88 within restored ponds in which accretion was calculated using the WARMER model for the USACE Low Curve

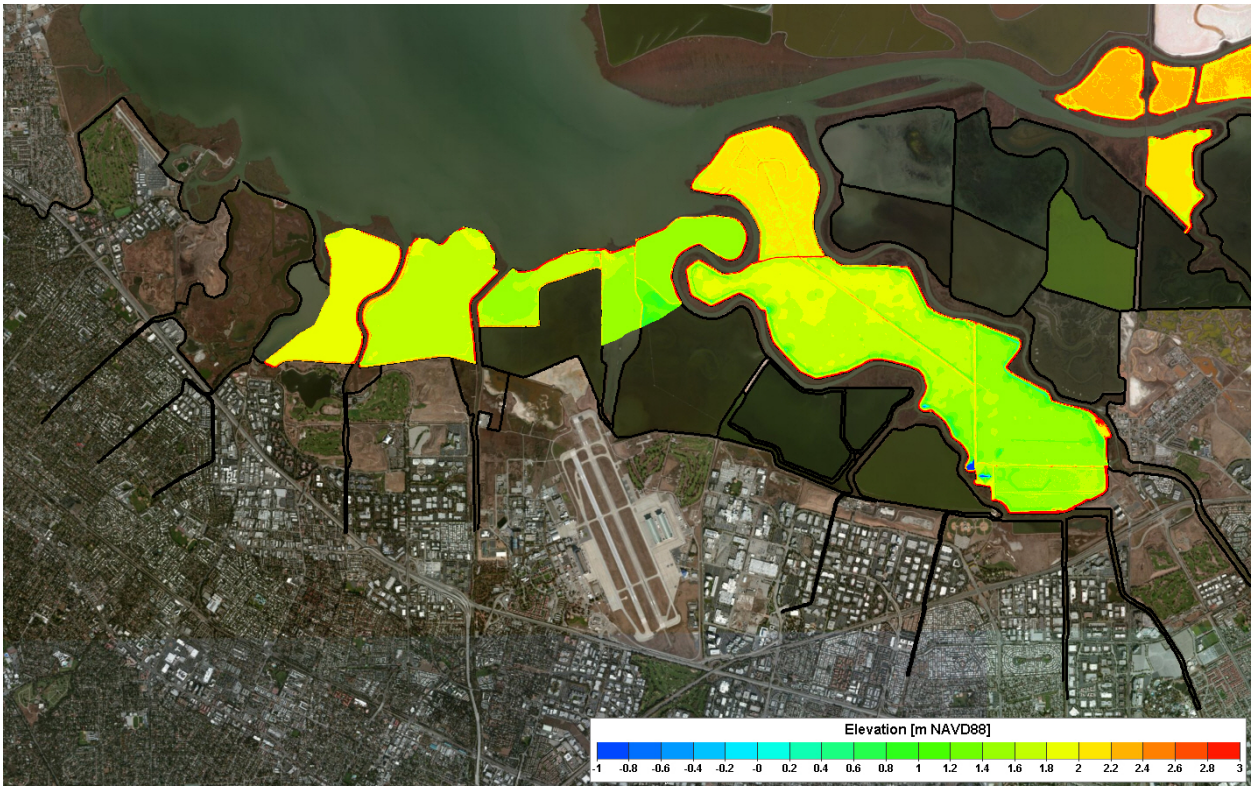

Figure 6.2-16

Final 2067 elevations in meters NAVD88 within restored ponds in which accretion was calculated using the WARMER model for the USACE Intermediate Curve

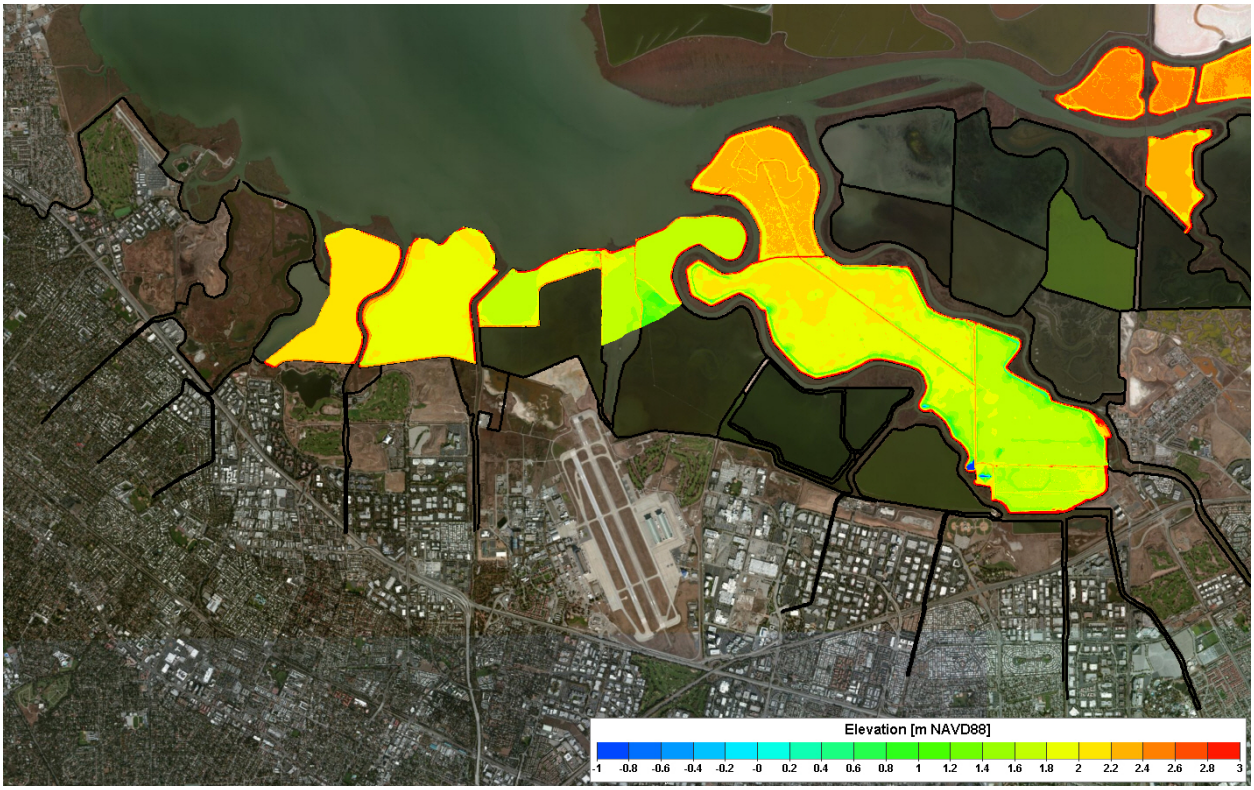

Figure 6.2-17

Final 2067 elevations in meters NAVD88 within restored ponds in which accretion was calculated using the WARMER model for the USACE High Curve

6.3 Water Surface Evaluation Locations for With-Project Scenarios

Predicted water surface elevations for each of the 144 Year 0 with-project scenarios and the 216 Year 50 with-project scenarios were evaluated at 69 locations spanning from EIA 1 through EIA 10 (Figure 6.3-1). Thirty-eight of the evaluation locations are located seaward of the proposed project levee alignment. Of these, fourteen evaluation stations are located immediately adjacent to the proposed project levee alignment. The remaining 31 evaluation locations are located behind the proposed project levee alignment to evaluate flood risk in each EIA behind the proposed project levee. For the with-project conditions, all of these 31 locations remain dry in the with-project scenarios, with the exception of the one point located within the PAFB. Because the PAFB is assumed to operate as a managed flood control basin in Year 50, the water surface elevation point inside the PAFB is wet even though the project levee does not overtop and there is no flooding behind the project levee.

For each scenario, lookup tables were developed to provide the maximum water surface elevation at each of the 69 locations for each of the 360 with-project scenarios simulated, resulting in a total of 24,840 predictions of maximum water surface elevations under with-project conditions. These predictions of maximum water surface elevation were used by Noble Consultants in the Monte Carlo simulations in order to develop the flood frequency curves at each of the 69 locations as part of this study. The results of these Monte Carlo simulations and the resulting flood frequency curves at each location are presented in a separate report by Noble Consultants.

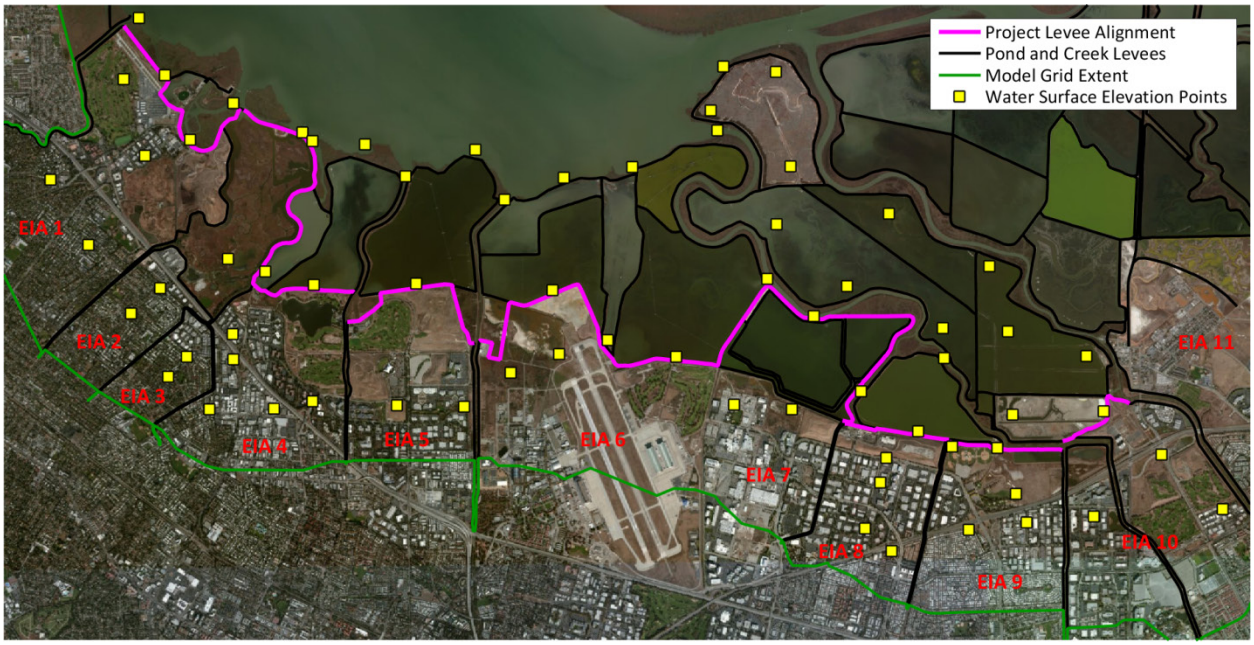

Figure 6.3-1

Locations used for evaluation of peak water surface elevations for the with-project scenarios. Black lines are creek and pond levees, the magenta line is the proposed project levee alignment, and the green line is the model grid extent.

7 SUMMARY AND CONCLUSIONS

The primary results of the long wave modeling study are the set of lookup tables which provide maximum water surface elevations at 69 locations for 1,080 model scenarios, resulting in 74,520 predictions of maximum water surface elevations for hydrodynamic conditions spanning a wide range of astronomical tides, storm surge, wind, levee failures, and SLR for both existing conditions and with-project conditions. These lookup tables were provided to Noble Consultants for the Monte Carlo analysis. Because the 1,080 scenarios and 74,520 individual water level predictions precludes a detailed explanation of each scenario or each predicted water level, this section presents a brief overview of the different sets of scenarios. The summaries present an overview of the results from the Year 0 existing conditions, Year 50 existing conditions, Year 0 with-project conditions, and Year 50 with-project conditions. These summaries provide a general overview of the effect of levee breaches, wind, SLR, and the project levee on predicted water levels in the study area. Additional discussion focused on specific locations within the study area is included in the report documenting the Monte Carlo simulations which was prepared by Noble Consultants.

7.1 Year 0 Existing Conditions

Under Year 0 existing conditions, there was no predicted flooding into EIAs 1-10 for the 0.5 ft and 1.5 ft surge events in any scenarios that did not include levee breaches. For the 2.5 ft surge events, overtopping of the existing levee near the confluence of Sunnyvale East, Calabazas Creek, and San Tomas Aquino Creek occurred into EIA 9. The confluence of the three creeks and the combined creek flows adjacent to EIA 9 is a large factor in the overtopping of the levee into EIA 9. In Event 12, the water overtopped the existing levee just south of San Francisquito Creek and flooded a small portion of EIA 1. The wind scenarios indicated that wind from the northwest increased the water surface elevations in the Far South Bay for all scenarios. In the scenarios with levee breaches, the scenarios with inner and outer levee breaches resulted in increased flooding into EIAs 1-9 landward of the breach locations.

7.2 Year 50 Existing Conditions

As expected, the inclusion of SLR in the Year 50 existing conditions scenarios increased the water surface elevations in the Far South Bay and increased the amount of levee overtopping

of the existing inner and outer levees. The results for the Year 50 existing conditions for the USACE Low Curve are similar to the Year 0 conditions with flooding into EIA 9 under the high surge events and into EIA 1 for Event 12. For the Year 50 existing conditions for the USACE Intermediate and High Curves, the number of events that experienced levee overtopping and the extent of landward flooding behind the levee is higher than for the USACE Low Curve. Under the USACE High Curve, all of the 2.5 ft surge events resulted in overtopping of the levee south of San Francisquito Creek into EIA 1. For Event 12 with the USACE High Curve and the highest simulated water level at the San Francisco NOAA station, a large amount of levee overtopping and flooding occurred in EIA 1, EIA 2, EIA 3, EIA 4, EIA 6, EIA 7, and EIA 9. The large amount of levee overtopping in the higher water level events for the scenarios that included the USACE High Curve resulted in the predicted water surface elevations landward of the proposed project levee alignment being relatively similar between the no-breach and with-breach conditions.

7.3 Year 0 With-Project Conditions

No flooding was predicted landward of the project levee for any of the Year 0 with-project condition scenarios. Because the project levee does not overtop and does not breach, a general increase in the water levels along the project levee relative to existing conditions was predicted for any scenarios where the existing conditions scenarios flooded into EIAs 1-10. This increase in the predicted water levels along the project levee is most pronounced near the confluence of Sunnyvale East, Calabazas Creek, and San Tomas Aquino Creek because the creek inflow cannot overtop the project levee into EIA 9. Because the predicted water levels at this location strongly influenced by the creek inflows, the water levels from the Monte Carlo simulations may underestimate the 100-year water levels along the creek levees in EIA 9 because creek inflows were less than the 100-year flows. Similarly, because the water levels inside PAFB are controlled by inflow from Matadero Creek, Adobe Creek, Barron Creek, and the capacity of the outlet structure to release flow at low water, the water surface elevations inside the PAFB predicted in this analysis should not be considered 100-year water levels inside the PAFB because the inflows to PAFB in the scenario simulations are considerably lower than 100-year flows (under all of the Year 0 and Year 50 conditions simulated).

7.4 Year 50 With-Project Conditions

No flooding was predicted landward of the project levee for any of the Year 50 with-project conditions. Both the pond restoration and the inclusion of the project levee had effects on the predicted water levels relative to the water levels for Year 50 existing conditions. Pond restoration and marsh accretion tended to reduce the predicted water levels at the water surface elevation locations bayward of the project levee. The project levee tended to increase the predicted water levels bayward of the project levee for scenarios where flooding into EIAs 1-10 occurred under Year 50 existing conditions.

Restoration of the salt ponds resulted in lower predicted water surface elevations near the confluence of Sunnyvale East, Calabazas Creek, and San Tomas Aquino Creek than under existing conditions in many scenarios. This reduction in the predicted water surface elevations is partially the result of the breach along the south levee of Pond A8S near the mouth of Calabazas Creek, which allows the creek flows to spread out into the restored ponds. However, for some of the Year 50 scenarios with high peak water levels, the surge from the Bay is high enough to reduce the effect of this breach on water levels adjacent to EIA 9.

ACKNOWLEDGEMENTS

This project is being conducted for the Santa Clara Valley Water District (SCVWD) under subcontract to Noble Consultants. The authors would like to thank Jen Men Lo (SCVWD), Emily Zedler (SCVWD), Rechelle Blanc (SCVWD), Raymond Wong (SCVWD), Errol Gabrielsen (SCVWD), Chia-Chi Lu (Noble Consultants, Inc.), John Bourgeois (South Bay Salt Pond Restoration Project), Eric Mruz (USFWS), Renée Spenst (Ducks Unlimited), Amy Foxgrover (USGS), and Laura Valoppi (USGS) for access to data and other information which was used for this project.

The high-resolution DEM of Far South Francisco Bay was developed by James Zoulas (USACE). The authors would like to acknowledge the tremendous effort that went into the development of this DEM in order to meet the datum compliance standards for the SSFBSS. The UnTRIM code was developed by Professor Vincenzo Casulli (University of Trento, Italy). The WARMER model was developed and applied by Kathleen Swanson. Lastly, the authors would like to thank Frank Wu (USACE, retired), for his comments and careful review of an earlier draft of this report.

REFERENCES

Allen, J. R. L., 1995. Salt-marsh growth and fluctuating sea level: implications of a simulation model for Flandrian coastal stratigraphy and peat-based sea-level curves. *Sedimentary Geology* 100(1): 21-45.

Callaway, J. C., J. A. Nyman, and R. D. DeLaune, 1996. Sediment accretion in coastal wetlands: a review and a simulation model of processes. *Current topics in wetland biogeochemistry* 2: 2-23.

Casulli, V., 1990. Semi-implicit finite difference methods for the two-dimensional shallow water equations. *Journal of Computational Physics* 86:56-74. Available from: http://dx.doi.org/10.1016/0021-9991(90)90091-E.

Casulli, V., 1999. A semi-implicit numerical method for non-hydrostatic free-surface flows on unstructured grid, in Numerical Modelling of Hydrodynamic Systems. ESF Workshop, p. 175-193, Zaragoza, Spain.

Casulli, V. and E. Cattani, 1994. Stability, accuracy and efficiency of a semi-implicit method for three-dimensional shallow water flow. *Computers and Mathematics with Applications* 27(4):99-112. http://dx.doi.org/10.1016/0898-1221(94)90059-0.

Casulli, V. and R.T. Cheng, 1992. Semi-implicit finite difference methods for three-dimensional shallow water flow. *International Journal for Numerical Methods in Fluids* 15:629-648. Available from: http://dx.doi.org/10.1002/fld.1650150602.

Casulli, V. and R.A. Walters, 2000. An unstructured, three-dimensional model based on the shallow water equations. *International Journal for Numerical Methods in Fluids* 32:331-348. Available from: http://dx.doi.org/10.1002/(SICI)1097-0363(20000215)32:3<331::AID-FLD941>3.0.CO;2-C.

Casulli, V. and P. Zanolli, 2002. Semi-Implicit Numerical Modelling of Non-Hydrostatic Free-Surface Flows for Environmental Problems. *Mathematical and Computer Modelling* 36:1131-1149. Available from: http://dx.doi.org/10.1016/S0895-7177(02)00264-9.

Casulli, V. and P. Zanolli, 2005. High Resolution Methods for Multidimensional Advection-Diffusion Problems in Free-Surface Hydrodynamics. *Ocean Modelling* 10 (1-2): 137-151. Available from: http://dx.doi.org/10.1016/j.ocemod.2004.06.007.

Cheng, R.T., V. Casulli, and J.W. Gartner, 1993. Tidal residual intertidal mudflat (TRIM) model and its applications to San Francisco Bay, California. *Estuarine, Coastal and Shelf Science* 369:235-280. Available from: http://dx.doi.org/10.1006/ecss.1993.1016.

Cheng, R.T. and V. Casulli, 1996. Modeling the Periodic Stratification and Gravitational Circulation in San Francisco Bay. Proceedings of 4th Inter. Conf. on Estuarine and Coastal Modeling, Spaulding and Cheng (Eds.), ASCE, San Diego, California, October 1995, 240-254.

Cheng, R.T. and V. Casulli, 2002. Evaluation of the UnTRIM model for 3-D Tidal Circulation. Proceedings of the 7th International Conference on Estuarine and Coastal Modeling, St. Petersburg, Florida, November 2001, 628-642.

Cheng, R.T. and R.E. Smith, 1998. A Nowcast Model for Tides and Tidal Currents in San Francisco Bay, California, Ocean Community Conf. '98, Marine Technology Society, Baltimore, Maryland, November 15 to 19, 1998, 537-543.

D'Alpaos, A., 2011. The mutual influence of biotic and abiotic components on the long-term ecomorphodynamic evolution of salt-marsh ecosystems. *Geomorphology* 126(3): 269-278.

Deleersnijder, E., J.M. Beckers, J.M. Campin, M. El Mohajir, T. Fichefet, and P. Luyten, 1997. Some mathematical problems associated with the development and use of marine models. In *The Mathematics of Models for Climatology and Environment*, Vol. 148, edited by J.I. Diaz. Springer Verlag, Berlin, Heidelberg. Available from: http://dx.doi.org/10.1007/978-3-642-60603-8_2.

French, J.R., 1993. Numerical simulation of vertical marsh growth and adjustment to accelerated sea-level rise, north Norfolk, UK. *Earth Surface Processes and Landforms* 18(1): 63-81.

French, J., 2006. Tidal marsh sedimentation and resilience to environmental change: exploratory modelling of tidal, sea-level and sediment supply forcing in predominantly allochthonous systems. *Marine Geology* 235(1): 119-136.

Gross, E.S., J.R. Koseff, and S.G. Monismith, 1999. Three-dimensional salinity simulations of South San Francisco Bay. *Journal of Hydraulic Engineering* 125(11):1199-1209. Available from: http://dx.doi.org/10.1061/(ASCE)0733-9429(1999)125:11(1199).

Gross, E.S., M.L. MacWilliams, and W. Kimmerer, 2006. Simulating Periodic Stratification in San Francisco Bay. Proceedings of the Estuarine and Coastal Modeling Conference, ASCE.

Hydroikos, Ltd., 2009. Operation of tide gates at Charleston Slough, Technical Memo, August 21, 2009.

Kantha, L.H. and C.A. Clayson, 1994. An improved mixed layer model for geophysical applications. *Journal of Geophysical Research* 99:25235–25266. Available from: http://dx.doi.org/10.1029/94JC02257.

Kirwan, M.L., and A.B. Murray, 2007. A coupled geomorphic and ecological model of tidal marsh evolution. *Proceedings of the National Academy of Sciences* 104(15): 6118-6122.

Kirwan, Matthew L. and G.R. Guntenspergen, 2012. Feedbacks between inundation, root production, and shoot growth in a rapidly submerging brackish marsh. *Journal of Ecology* 100(3): 764-770.

Letter, C. and A.K. Sturm, 2010. *Long wave modeling for South San Francisco Bay Shoreline Study: Without Project Conditions*. ERDC/CHL Draft Final Report. May 2010.

Lippert, C. and F. Sellerhoff, 2007. Efficient Generation of Unstructured Orthogonal Grids, The 7th Int. Conf. on Hydroscience and Engineering (ICHE-2006), Sep. 10 – Sep. 13, Philadelphia, USA.

MacWilliams, M.L. and R.T. Cheng, 2007. Three-dimensional hydrodynamic modeling of San Pablo Bay on an unstructured grid. The 7th Int. Conf. on Hydroscience and Engineering (ICHE-2006), Philadelphia, Pennsylvania, September 10 to September 13, 2007.

MacWilliams, M.L. and E.S. Gross, 2007. *UnTRIM San Francisco Bay-Delta Model Calibration Report, Delta Risk Management Study.* Prepared for California Department of Water Resources. March 2007.

MacWilliams, M.L., E.S. Gross, J.F. DeGeorge, and R.R. Rachiele, 2007. Three-dimensional hydrodynamic modeling of the San Francisco Estuary on an unstructured grid, IAHR. 32nd Congress, Venice Italy, July 1 to 6, 2007.

MacWilliams, M.L., F.G. Salcedo, and E.S. Gross, 2008. *San Francisco Bay-Delta UnTRIM Model Calibration Report, POD 3-D Particle Tracking Modeling Study.* Prepared for California Department of Water Resources. December 19, 2008.

MacWilliams, M.L., F.G. Salcedo, and E.S. Gross, 2009. *San Francisco Bay-Delta UnTRIM Model Calibration Report, Sacramento and Stockton Deep Water Ship Channel 3-D Hydrodynamic and Salinity Modeling Study.* Prepared for U.S. Army Corps of Engineers, San Francisco District. July 14, 2009.

MacWilliams, M.L., N.E. Kilham, and A.J. Bever, 2012. *South San Francisco Bay Long Wave Modeling Report*. Prepared for U.S. Army Corps of Engineers, San Francisco District. June 2012.

MacWilliams, M.L., A.J. Bever, E.S. Gross, G.A. Ketefian, and W.J. Kimmerer, 2015. Three-Dimensional Modeling of Hydrodynamics and Salinity in the San Francisco Estuary: An Evaluation of Model Accuracy, X2, and the Low Salinity Zone. *San Francisco Estuary and Watershed Science* 13(1): 37. Available from: http://dx.doi.org/10.15447/sfews.2015v13iss1art2.

Morris, J.T., P.V. Sundareshwar, C.T. Nietch, B. Kjerfve, and D.R. Cahoon, 2002. Responses of coastal wetlands to rising sea level. *Ecology* 83(10): 2869-2877.

Mruz, E. and J. Bourgeois, 2014. Personal communication with M.L. MacWilliams. Santa Clara, CA. July 3, 2014.

Noble Consultants, 2009. *San Francisquito Creek Development and Calibration/Verification of Hydraulic Model*. Final Report. Prepared for U.S. Army Corps of Engineers, San Francisco District. May 2009.

Noble Consultants, 2015. *Hydraulic Analysis for Preliminary Feasibility Study in Economic Impact Areas 1 to 10 along South San Francisco Bay Shoreline, California*. Report. Prepared for Santa Clara Valley Water District. September 2015.

Schaaf & Wheeler, 2005. *Operations Plans for Alviso Low Salinity Salt Ponds*. Available from: http://www.southbayrestoration.org/pdf_files/Operations%20Plans%20Alviso%20May%202005.pdf

Schaaf & Wheeler, 2014. Palo Alto Flood Basin Hydrology, Final Report. Prepared for Santa Clara Valley Water District. July 2014.

Swanson, K.M., J.Z. Drexler, D.H. Schoellhamer, K.M. Thorne, M.L. Casazza, C.T. Overton, J.C. Callaway, and J.Y. Takekawa, 2014. Wetland accretion rate model of ecosystem resilience (WARMER) and its application to habitat sustainability for endangered species in the San Francisco Estuary. *Estuaries and Coasts* 37(2): 476-492.

Swanson, K.M., J.Z. Drexler, C.C. Fuller, and D.H.Schoellhamer, 2015. Modeling Tidal Freshwater Marsh Sustainability in the Sacramento–San Joaquin Delta Under a Broad Suite of Potential Future Scenarios. *San Francisco Estuary and Watershed Science* 13(1). Available from: http://escholarship.org/uc/item/9h8197nt.

Umlauf, L. and H. Burchard, 2003. A generic length-scale equation for geophysical turbulence models. *Journal of Marine Research* 61:235–265. http://dx.doi.org/10.1357/002224003322005087.

USACE (U.S. Army Corps of Engineers), 2010. *Riverine Hydraulic Analysis for South San Francisco Bay shoreline Study, Santa Clara & Alameda Counties, California: Without Project Conditions*. USACE, San Francisco District. March 2010.

USACE, 2013. *Incorporating Sea Level Change in Civil Works Programs*. ER 1100-2-8162. Regulation No. 1100-2-8162. Available from: http://www.publications.usace.army.mil/Portals/76/Publications/EngineerRegulations/ER_1100-2-8162.pdf

USACE, 2014. Sea-Level Change Calculator. Cited: November 2014. Available from: http://corpsclimate.us/ccaceslcurves.cfm.

USFWS (United States Fish and Wildlife Service), 2015. *2014 Annual Self-Monitoring Report, Don Edwards San Francisco Bay National Wildlife Refuge, Fremont, California*. Revised April 10, 2015. Available from: http://www.southbayrestoration.org/monitoring/Revised%20Final%20Annual%20Self-Monitoring%20Report_4.10.15%20.pdf.

Warner J.C., C.S. Sherwood, H.G. Arango, and R.P. Signell, 2005. Performance of four turbulence closure models implemented using a generic length scale method. *Ocean Modeling* 8:81-113. Available from: http://dx.doi.org/10.1016/j.ocemod.2003.12.003.

Williams P.B. and M.K. Orr, 2002. Physical evolution of restored breached levee salt marshes in the San Francisco Bay estuary. *Restoration Ecology* 10: 527-542.